BRIGHAM

YOUNG

UNIVERSITY

GEOLOGY STUDIES

Volume 23, Part 1—October 1976

CONTENTS

Brigham Young University Geology Studies

Volume 23, Part 1—October 1976

Contents

A publication of the
Department of Geology
Brigham Young University
Provo, Utah 84602

Editor

W. Kenneth Hamblin

Brigham Young University Geology Studies is published semiannually by the department. *Geology Studies* consists of graduate-student and staff research in the department and occasional papers from other contributors. *Studies for Students* supplements the regular issues and is intended as a series of short papers of general interest which may serve as guides to the geology of Utah for beginning students and laymen.

ISSN 0068-1016

Distributed September 15, 1976

Price $5.00

(Subject to change without notice)

9-76 600 13879

Paleoenvironments of the Upper Entrada Sandstone and the Curtis Formation on the West Flank of the San Rafael Swell, Emery County, Utah*

LARRY S. SMITH
Continental Oil Company, Houston, Texas

ABSTRACT.—Transgressive and regressive phases of two major Late Jurassic epicontinental seas into east central Utah are documented by sediments of the upper Entrada Sandstone and the Curtis Formation.

Sediments of the Entrada Sandstone, predominantly red beds, reflect marine regression and sedimentation in four subenvironments within a complex coastal-interdeltaic depositional system. These subenvironments denote low-energy, shallow water sedimentation and are represented by four primary facies: (1) a cyclic red mudstone and sandstone facies, (2) a thick red sandstone and siltstone facies, (3) a thin, large-scale, cross-bedded, sandstone facies, and (4) a thin green sandstone facies.

Cyclic deposition of red sandstone and mudstone characterizes the first facies. Associated sedimentary structures such as channels, current, wave, and climbing ripple marks, deformation structures, mud cracks, and lenticular sandstone bodies suggest tidal, possible deltaic, storm and flooding, and active biologic processes during deposition.

The thick red sandstone and siltstone facies dominates the section and is characterized by the occurrence of syngenetic chert, deformed internal stratification, current and wave-generated ripple marks, climbing ripple marks, and limited deposition of mud.

The thin third primary facies is a sandstone characterized by large-scale, trough-shaped crossbed sets. Units of this facies are relatively thin and occur only twice in the section.

The thin green sandstone facies characterizes two relatively thin units of the section.

The vertical sequence of strata in the Entrada section reflects a repetitious occurrence of these four facies, and records two brief transgressive marine phases represented by sediments of the green sandstone and cross-bedded sandstone facies, and three regressive phases represented by the thick red sandstone and siltstone and cyclic red mudstone and sandstone facies.

Green rocks of the Curtis Formation unconformably overlie rocks of the Entrada Sandstone and record a complete cycle of transgression and regression of the final major Late Jurassic (Oxfordian) epeiric sea into the area of study. The 65-meter section is divisible into four main facies: (1) a thin basal conglomerate facies. (2) a lower facies dominated by claystone with thin siltstone interbeds, (3) a middle facies dominated by glauconitic sandstone, and (4) an upper facies dominated by clayey siltstone with thin sandstone interbeds.

Sediments of the two lower facies of the Curtis Formation represent the transgressive phase of the seaway over previously emergent areas. They reflect the initial inundation resulting in the formation of the basal lag deposit, followed by slow, nearly continuous deposition of fine clastic marine sediment.

Glauconitic sandstone of the middle facies was deposited as a broad, widespread sand sheet and represents deposition during static and regressive phases of the Oxfordian seaway.

Dominant marine Curtis sedimentation ceased with regression of the sea. Fine clastic sediments of the upper facies represent the transition from a marine environment to deposition in a tidal flat environment recorded by sediments of the overlying Summerville Formation.

*A thesis presented to the Department of Geology, Brigham Young University, in partial fulfillment of the requirements for the degree Master of Science, April 1976. J. Keith Rigby, thesis chairman.

CONTENTS

INTRODUCTION

Upper Jurassic reddish Entrada Sandstone (Callovian) and greenish Curtis Formation (Oxfordian) are two environmentally and lithologically distinct sequences of rocks. In gross aspects they are the products of transgressive and regressive pulses of major Late Jurassic epicontinental seas which invaded the western interior of the United States. The formations are both lithologically and visually distinct and produce some of the interesting scenery of the San Rafael Swell.

Excellent exposures provided by road cuts of Interstate 70 allow documentation and interpretation of this Jurassic sedimentary sequence. Detailed study of the vertical progression of sediments representing varied environments

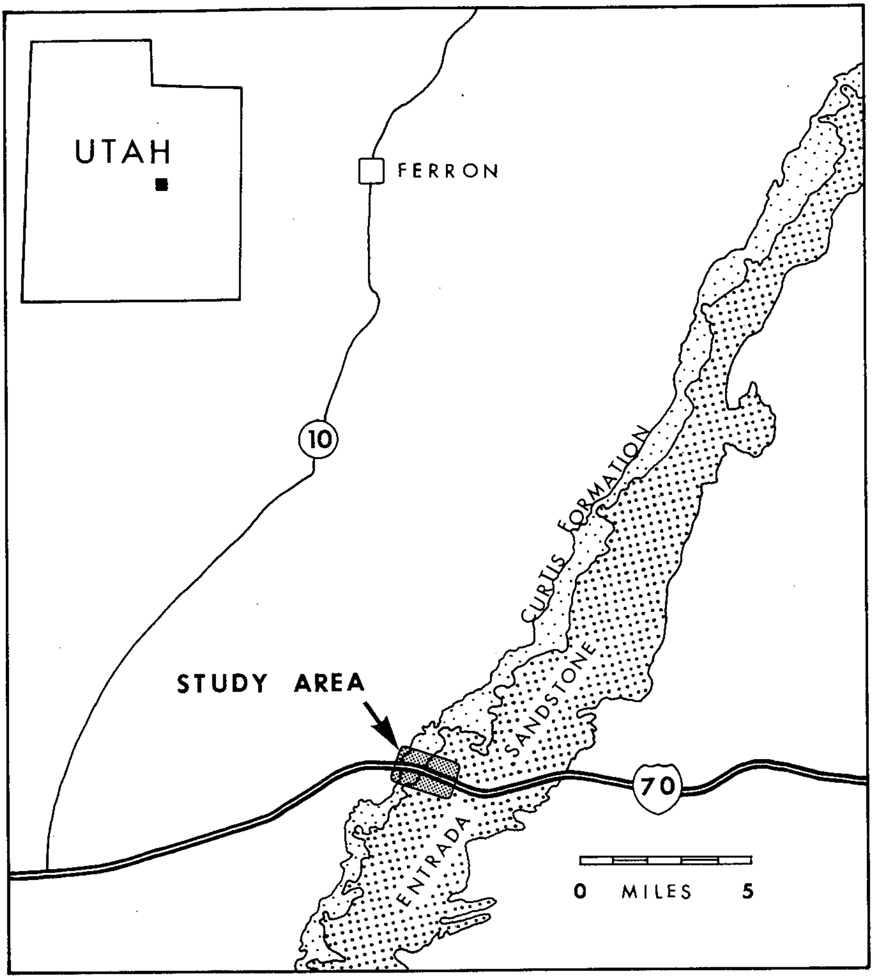

TEXT-FIGURE 1.—Index map.

of deposition permits interpretation of the paleoenvironments and allows development of a model of the depositional histories of this sequence of rocks.

Location

The study area is located on the west flank of the San Rafael Swell in Sec. 11, T. 23 S, R. 6 E, in the Mesa Butte Quadrangle, Emery County, Utah (Text-fig. 1). Excellent exposures are provided in road cuts along the north and south sides of Interstate 70. Detailed sections of the upper Entrada Sandstone and of the Curtis Formation were measured both in the road cuts and in adjacent off-the-road exposures.

Geologic Setting

The Curtis Formation is considered by Imlay (1948, p. 17) to be in the *Cardioceras cordiforme* ammonoid faunal zone which is correlated with the lower Oxfordian of Europe. Imlay (1952, p. 960-962) correlated the Curtis Formation with other units such as the Stump Sandstone of southeastern Idaho and the Swift Formation of west central Montana. The Curtis Formation and its equivalents represent Upper Jurassic (Oxfordian) sediments deposited in part of an epicontinental seaway (Text-fig. 3) which extended south from the present Arctic (Brenner and Davies, 1974). This pulse was the last major transgressive-regressive Jurassic marine cycle across the Rocky Mountain Province.

The Curtis Formation unconformably overlies the Upper Jurassic (Callovian) red bed facies of the Entrada Sandstone in the study area. Sedimentation during Curtis time commenced with a marine invasion over previously emergent areas whose depositional record is represented by Entrada sediments. Assignment of the Entrada Sandstone to the Callovian faunal zone was based upon its stratigraphic position (Baker, Dane, and Reeside, 1936, p. 58).

Regression of the Curtis Sea during late Oxfordian time was accompanied by deposition of a tidal flat facies, the Upper Jurassic Summerville Formation. In the study area the Curtis Formation is overlain conformably by Summerville sediments.

Previous Work

Early workers of Jurassic stratigraphy in the western United States defined the Entrada Sandstone and the Curtis Formation as members of the San Rafael Group. These units have generally been the subjects of regional studies and have not been individually studied in detail on location.

The Entrada Sandstone was named by Gilluly and Reeside (1928, p. 76) from good exposures at Entrada Point, in the northern part of the San Rafael Swell. Here the Entrada Sandstone is a thick series of earthy sandstones and subordinate shales. The Curtis Formation of Late Jurassic age was named by Gilluly and Reeside (1928, p. 78) from exposures at Curtis Point, near the head of Cottonwood Springs Wash, on the northeast side of the San Rafael Swell. The Curtis formation is typically a greenish gray, glauconitic sandstone and shale with a coarse basal conglomerate.

Baker, Dane, and Reeside (1936) made regional stratigraphic correlations of the Entrada Sandstone and the Curtis Formation, outlined the distribution of these rock bodies with isopach maps, and offered paleodepositional interpretations. They recognized the intimate association of marine invasions with the genesis of both the Entrada and Curtis formations. The eastern sandstone facies of the Entrada Sandstone was considered a product of an eolian environment, while the well-bedded, red sandstone and siltstone facies, the Entrada of the San Rafael Swell, was interpreted as a marginal marine facies (Baker, Dane, and Reeside, 1936, p. 54). The Curtis Formation was thought to represent near-shore marine sedimentation. The most significant contribution to the reconstruction of the paleodepositional environments of the Curtis Formation and of the Entrada Sandstone was Imlay's (1957) treatise on the regional paleoecology of the Jurassic seas.

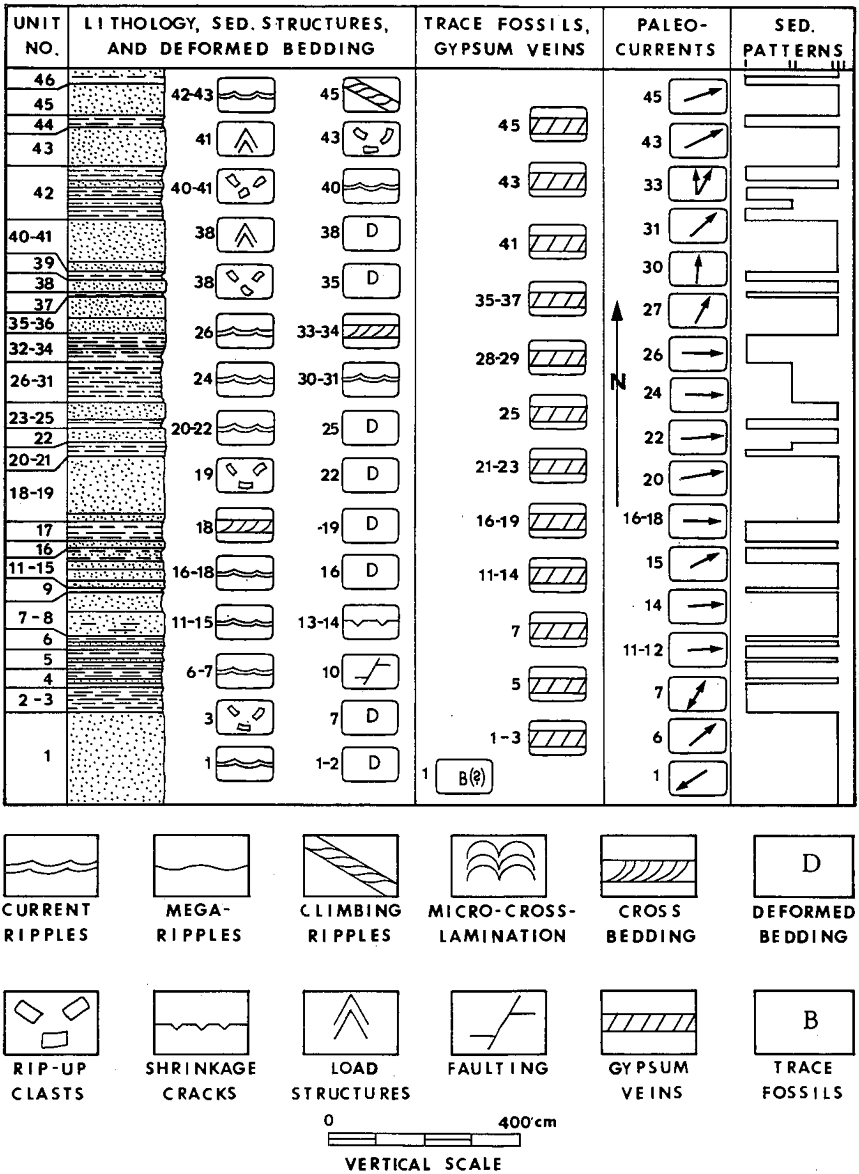

EXPLANATION OF TEXT-FIGURES

TEXT-FIGURE 2a.—Total studied stratigraphic section showing lithology. Sedimentary structures, gypsum veins, trace fossils, and paleocurrent directions are keyed to the stratigraphic units. Sedimentary pattern refers to occurrence of (1) mudstone, (II) siltstone, (III) sandstone.

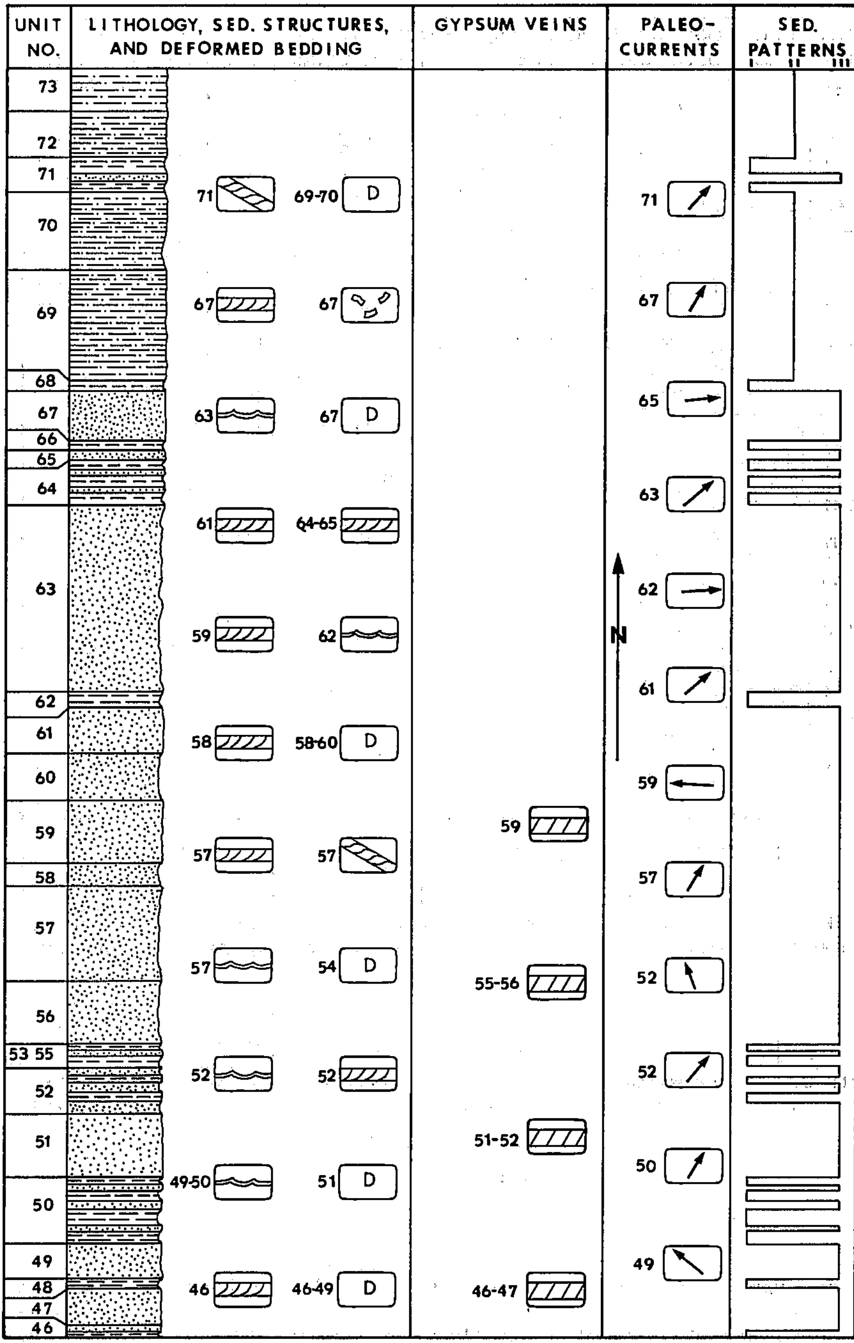

2b.—Stratigraphic section (Continued).

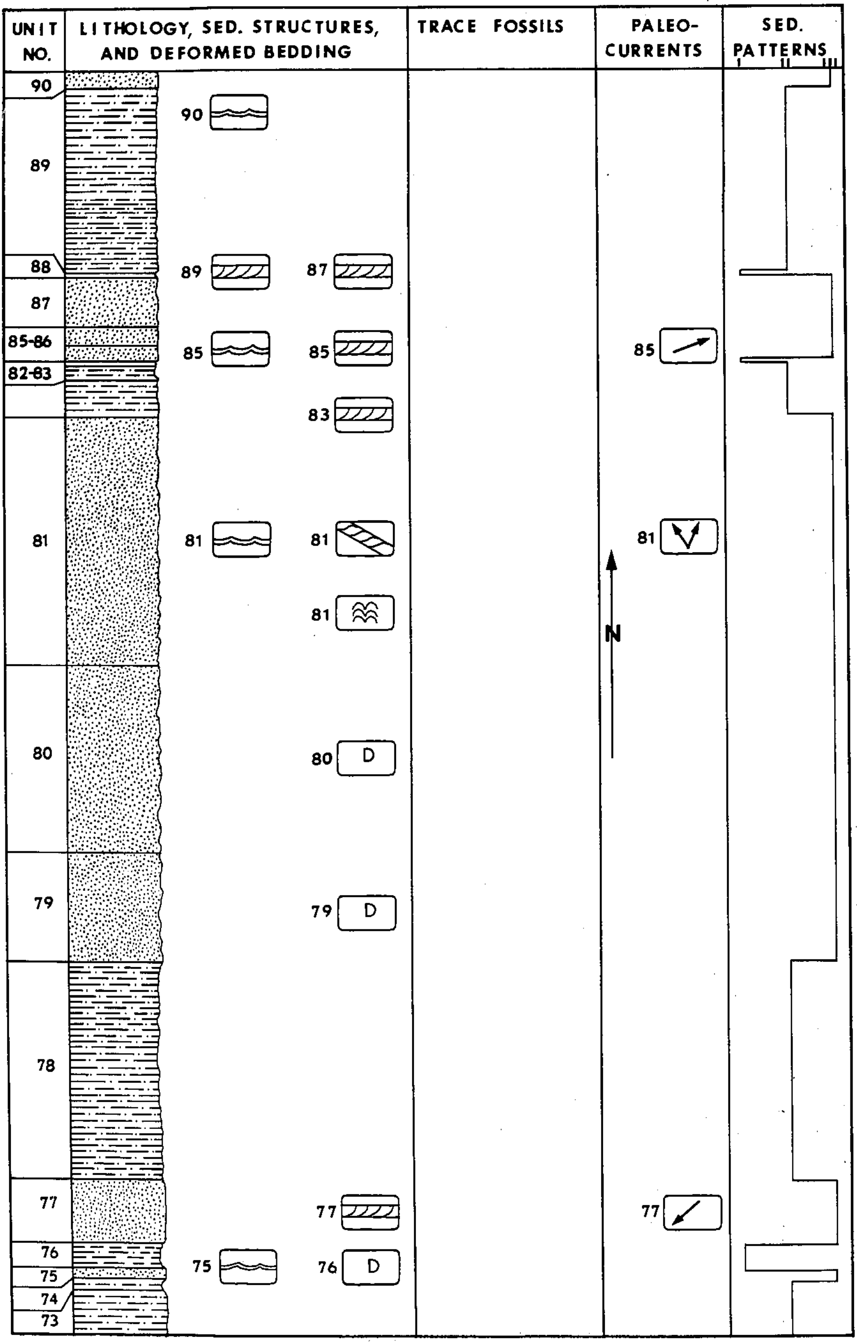

2c.—Stratigraphic section (Continued).

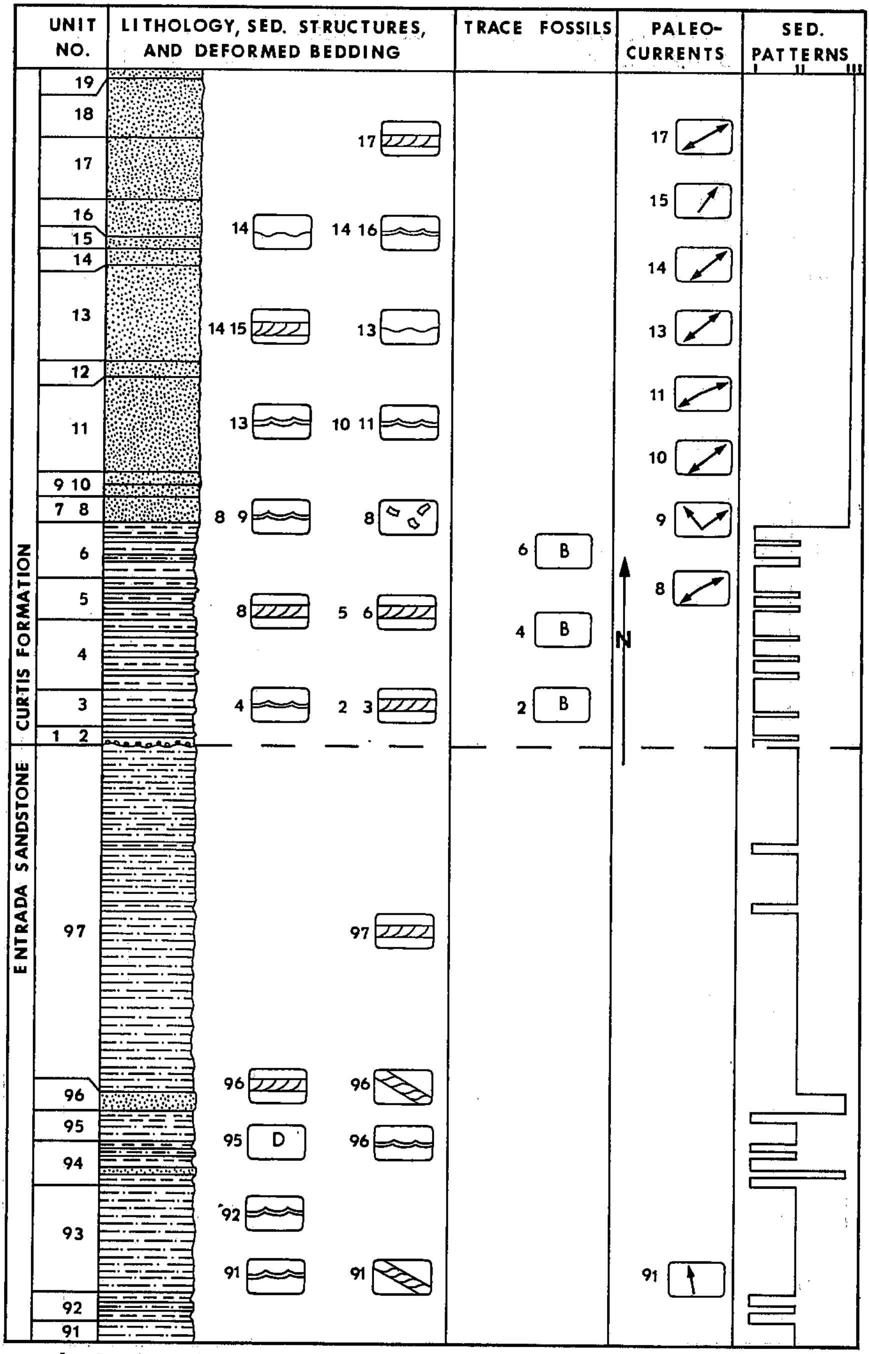

2d.—Stratigraphic section (Continued).

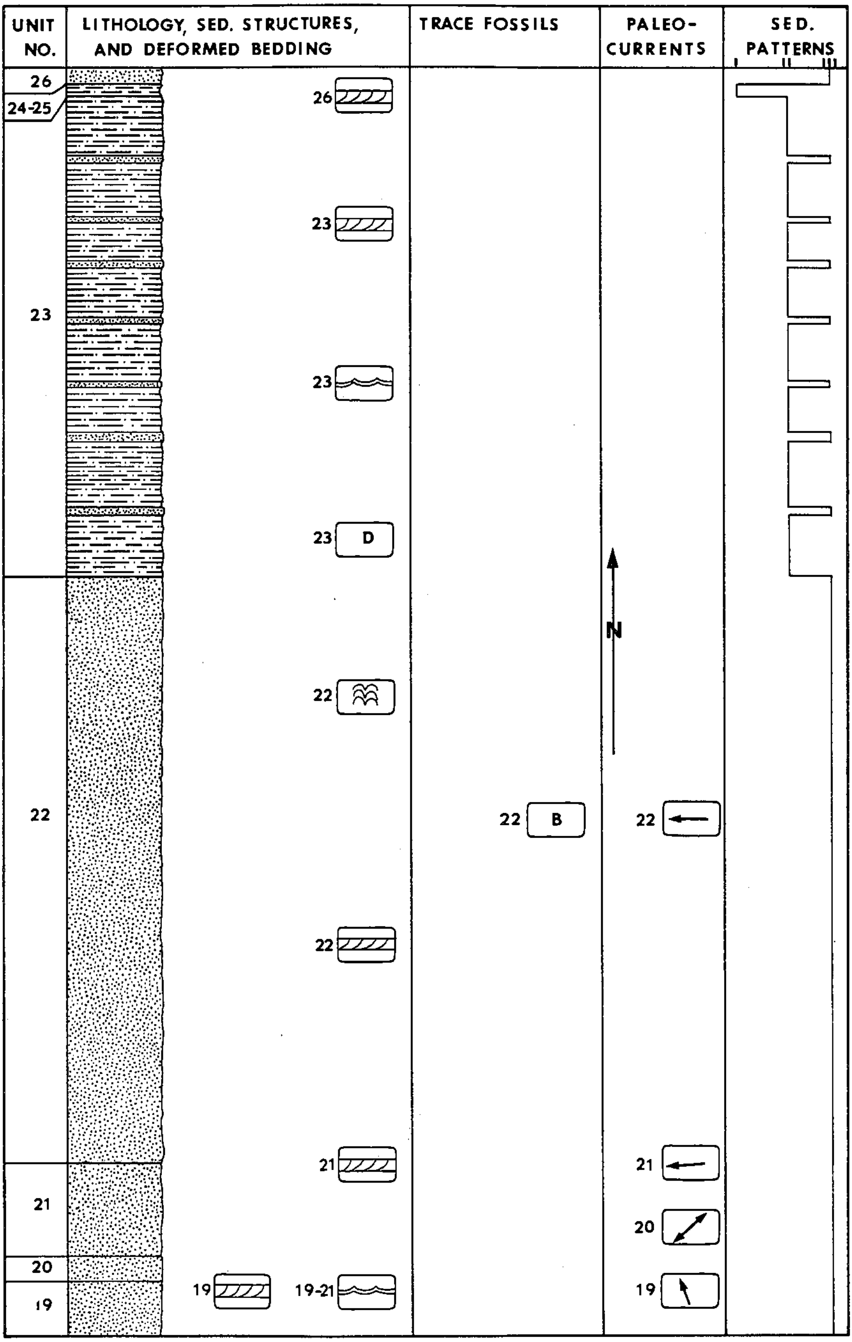

2e.—Stratigraphic section (Continued).

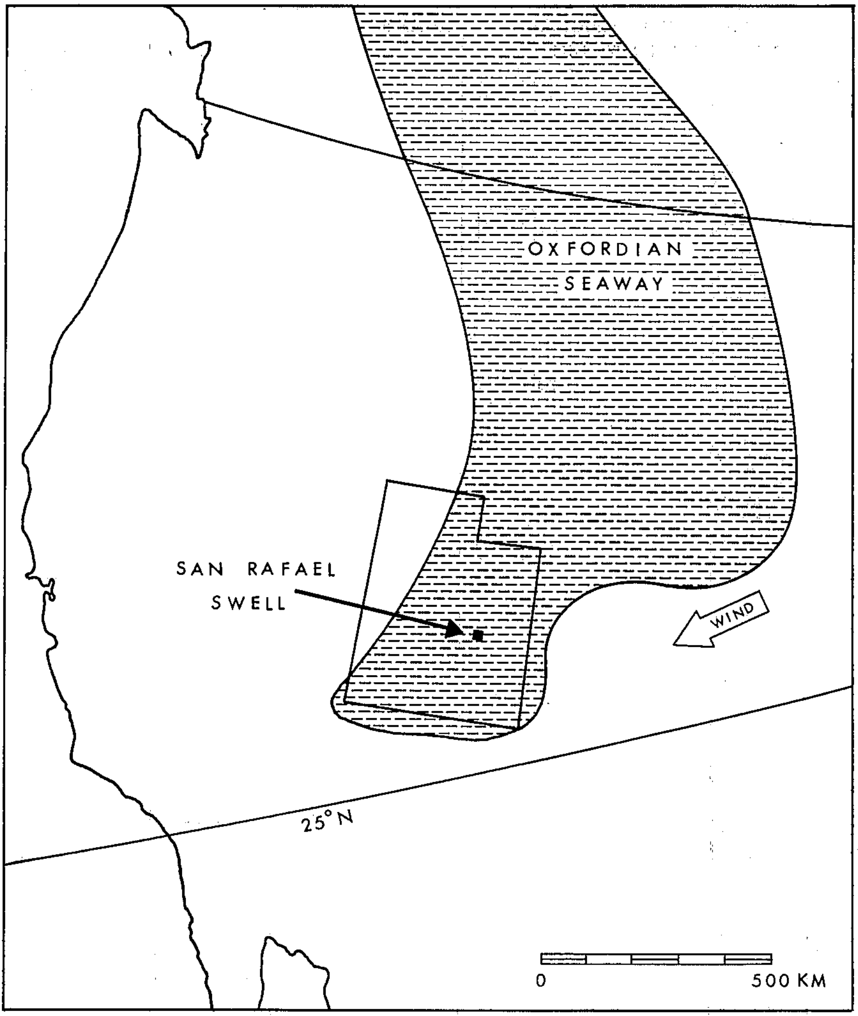

TEXT-FIGURE 3.—Paleogeographic map of Late Jurassic seaway modified from Miller (1952), and postulated Late Jurassic wind direction (after Tanner, 1965).

Methods of Study

The upper section of the Entrada Sandstone and a section of the Curtis Formation were measured in Interstate 70 roadcuts and adjacent exposures. These sections were measured in detail on a centimeter-by-centimeter scale and were subdivided into units based upon lithologic and sedimentary characteristics.

Attitudes of ripple marks and cross-bedding were measured with a Brunton compass on a unit-by-unit basis to determine paleocurrent trends. Paleocurrent maps were drawn for graphic representation of paleocurrent motion.

Field descriptions of individual units were recorded, either by means of a portable cassette tape recorder or in a field notebook. Sedimentary parameters analyzed include thickness, composition, clastic grain size, color, bedding, structures, and biologic features. Hand samples were collected from each unit for thin section analysis.

Large, 2x3-inch, thin sections were made of selected lithologies from the Entrada Sandstone and the Curtis Formation and examined under a petrographic microscope. Selected thin sections were stained with potassium ferricyanide and alizarine red S to distinguish between dolomite and calcite (Friedman, 1959, p. 95). Slabs were prepared, etched, and stained for the identification of potassium and plagioclase feldspar (Bailey and Stevens, 1960, p. 1025).

Nomenclature

Descriptive grain-size terminology used is the modified Wentworth grade scale proposed by Dunbar and Rodgers (1966, p. 161). Colors were described utilizing the Rock-Color Chart prepared by the Rock-Color Chart Committee and distributed by the Geological Society of America (1970).

Acknowledgments

The author deeply appreciates the guidance, counsel, and assistance of Dr. J. Keith Rigby who suggested the problem and served as thesis chairman. Thanks are extended to Dr. W. Kenneth Hamblin who served as committee member and offered critical advice and to Dr. H. J. Bissell for his helpful comments. Special thanks are due my wife, Laura, for her constant support and encouragement. Fellow graduate students Ron Lowrey, Allen Peterson, Gary Astin, and Bob Stanton gave freely of their time and equipment.

Financial assistance was provided by a grant-in-aid from the Research Committee of the American Association of Petroleum Geologists.

ENTRADA SANDSTONE

Terrigenous clastic rocks comprise the entire stratigraphic section of the Entrada Sandstone on the west flank of the San Rafael Swell. Adjacent to and within the study locality, the Entrada Sandstone is approximately 170 meters thick. This discussion will be concerned only with the upper 125 meters of the section (Text-figs. 2a, 2b, 2c, and 2d; Appendix 1).

Lithologies of the Entrada Sandstone

Rock types in the measured section of the Entrada Sandstone include mudstone, siltstone, and sandstone. Mudstone occurs in thirty-three of the ninety-seven units of the section, siltstone occurs in nineteen units, and sandstone occurs in forty-eight of the ninety-seven units described (Appendix 1). All but eleven units of the studied section are red beds.

Mudstone

The term *mudstone* is used in this study for fine-grained rocks composed of clay or fine silt and lacking fissility. Mudstones in the Entrada Sandstone form recessive units, some of which are prominent marker beds, particularly those exposed in the road cuts. These mudstone units range in thickness from 5 cm to 210 cm. Thin units are entirely of mudstone, while thicker units are interlayered with siltstone or sandstone beds.

Mudstone in the study section is grayish red to moderate reddish brown, and typically displays a nodular or flaky weathering habit. Mudstone units are generally well stratified; however, some units show evidence of soft-sediment deformation. Gypsum veins occur in Units 2, 3, 5, 13, and 23. Mud cracks are found in Unit 13.

Siltstone

Siltstone occurs at various intervals throughout the measured section and is of two types: (1) light reddish brown to pale red, and (2) pale green to grayish green. Light brownish gray and grayish red siltstone beds also occur, but infrequently.

Light reddish brown to pale red siltstone.—Light reddish brown to pale red siltstone occurs in sixteen of the nineteen siltstone units in the measured section and these units range in thickness from 3 cm to 1100 cm. Grain size in these units varies from 1/16 mm to 1/64 mm, coarse to fine silts. Some of these units contain very fine to sand-sized fine minerals, mostly quartz grains, in small amounts. Fragments and lenses of clay occur in some units. Quartz, potassium feldspar, plagioclase feldspar, and muscovite are the most commonly occurring minerals, with dolomite and calcite as accessory minerals. Units 30, 79, 80, and 95 are dolomite cemented.

Ripple marks or small-scale cross-lamination occur in one half of the siltstone units, with those in the lower part of the section showing current motion toward the northeast, and siltstone beds in the upper part of the section showing current motion toward the northwest. Deformed internal stratification occurs in Units 80, 95, and 97 (Pl. 3, figs. 2 and 3). Masses or stringers of red and white chert occur in Units 78 and 89. Gypsum veins are found in Unit 29 and occur parallel to the bedding.

Pale green to grayish green siltstone.—Green siltstone occurs in Unit 28 as alternating thin beds separated by mudstones, and in Units 70, 72, and 74 as confused, contorted lenses incorporated into grayish red siltstone or mudstone. Red and white chert masses or blebs are found associated with the greenish siltstone in Units 70 and 72. Internal stratification of Units 70, 72, and 74 is disrupted with evidence of bioturbation, rooting, or soft-sediment deformation (Pl. 3, fig. 1).

Light brownish gray and grayish red siltstones are minor and occur within other siltstone units. The mineralogy and sedimentary characteristics of these siltstones are similar to the pale green and light reddish brown units.

Sandstone

Sandstone is the dominant lithology in the measured section and occurs with three main colors which are indicative of different sedimentary environments. These sandstones are: (1) pale reddish brown, (2) pale brown, (3) light olive gray.

Pale reddish brown sandstone.—Pale reddish brown sandstone is the most common sandstone found in the measured section. Grain size of these sandstone units varies from 1 mm to 1/16 mm in diameter, coarse to very fine sand, with the average grain size approximately 1/8 mm. Sandstone of the formation is composed primarily of detrital quartz, potassium feldspar, and plagioclase feldspar, with minor amounts of calcite and dolomite clastic grains and organic fragments.

The pale reddish brown sandstones are friable, calcite cemented, and moderately to poorly sorted. Gypsum veins occur in many units of this rock type in the lower part of the section. Red and white chert occurs in the sandstone in Units 1, 69, and 79. The internal stratification of many of these units is distorted or destroyed, possibly due to bioturbation or rooting. Soft-sediment loading structures are found in the basal parts of Units 38, 41, and 47. Rip-up clasts occur in Units 19, 38, 40 through 43, and 49. Ripple marks and crossbeds are common throughout the sandstone units. Mud cracks occur in Unit 14. The reddish color of these sandstones and their associated sedimentary structures suggest an oxidizing environment with periodic subaerial exposure.

Pale brown sandstone.—Pale brown sandstone occurs only in Unit 77 where it is 200 cm thick. Grain size of this sandstone varies from $1\frac{1}{2}$ mm to $\frac{1}{4}$ mm, very coarse to medium sand. This sandstone is composed of detrital quartz, potassium feldspar, plagioclase feldspar, chert, and dolomite. Smaller grains are subangular to subrounded, whereas the coarser fraction is subrounded to well rounded.

The sandstone is friable, calcite cemented, and poorly sorted. Weathered remnants of clay clasts occur in the lowermost part of the unit, which has an undulatory base.

Unit 77 forms a prominent resistant ledge and is characterized by large-scale crossbed sets whose thickness is that of the entire thickness of the unit. Crossbed foresets are defined in the unit by the coarser grains which give the rock a graded appearance in vertical section. Paleocurrent motion here was toward the southwest.

Light olive gray sandstone.—Light olive gray to light greenish gray sandstone occurs in Units 6, 9, 57, 58, and 75. Sandstone in Units 6 and 9 is interbedded with mudstone and thicknesses of the sandstone layers vary from 1 cm to 5 cm. Sandstone is 300 cm thick in Unit 57 and 75 cm thick in Unit 58, with interbedded mudstones. Sandstone in Unit 75 is 35 cm thick. Grain size of these sandstones varies from $\frac{1}{4}$ to 1/16 mm in diameter, fine to very fine sand. These sandstone units are composed primarily of quartz, potassium and plagioclase feldspar, with muscovite comprising 5 percent of the grains in Unit 75. The color of the beds suggests a reducing, perhaps subaqueous, environment.

Green sandstones, cemented with calcite and some dolomite, are moderately indurated, and moderately sorted. Ripple marks and cross-lamination are found in these units.

Evaporite Deposits in Entrada Sediments

Evaporite deposits encountered in the measured section of the Entrada Sandstone consist of veins, veinlets, and thin lenses of fibrous gypsum, and are restricted to the lower 59 units. These fibrous gypsum veins are usually less than 1 cm thick. Locally, however, veins up to 3 cm thick occur in Unit 12. Length of individual veins is quite variable. Some are only a few centimeters long, but others extend several meters or tens of meters along the road cuts where exposures are excellent. Selenite crystals were found only in the top of Unit 52.

Veins, veinlets, and lenses of gypsum occur in 33 of the lower 59 Entrada units and are not restricted to any particular lithology. Gypsum was found in 21 sandstone units, 9 mudstone units, and 3 siltstone units.

Typically, gypsum veins develop parallel or subparallel to internal stratification, if present, or with the upper and lower contacts of the unit in which they occur (Pl. 1, fig. 5). Veins cut across stratification at steep angles in Units 35, 46, and 49. Complex interweaving of gypsum veinlets characterize some units, such as Units 18, 25, 41, 45, 46, 47, and 51. Gypsum veinlets in these units commonly split into two or more branches, then intersect, outlining lenses of sediment in cross section.

Structurally, the veins are of two types, those with a median suture line, and those without. All are composed of fibrous gypsum (satin spar) with the crystal fibers extending transverse to the long axis of the veins. Gypsum veins exhibiting both types of structure occur in the same units, and microveins showing both structural types are found in the same thin section.

A median suture perhaps indicates either gypsum crystal growth initiated both on the upper and lower walls of preexisting fissures or permeable zones and continued inward until the opposite sides met, or that crystal growth initiated at a common point and extended outward in both directions.

Murray (1964), in a study of the origin and diagenesis of evaporites, concluded that gypsum may be the common, if not the universal, original calcium sulfate mineral. Field observations, such as those subsequently outlined, indicate that the origin of gypsum veins in the measured Entrada section is primary, and that the time of emplacement and crystallization of the gypsum was perhaps syndiagenetic (penecontemporaneous with diagenesis). No gypsum is found filling joints, so the time of emplacement must be prejointing. The joint system is most likely a postdiagenetic feature, perhaps related to the tectonic evolution of the San Rafael Swell. Other evidences suggesting a syndiagenetic origin are primarily crosscutting relationships between gypsum veins and sedimentary features assumed to be primary or penecontemporaneous with deposition, their normal parallelism with stratification, and general confinement within lithologic boundaries.

Gypsum veins are observed: (1) dissecting penecontemporaneous deformation structures in Units 38, 41, and 47 (Pl. 2, figs. 3, 4, and 6), (2) dissecting blocks of sediment rotated and deformed while in a semiconsolidated state (Pl. 2, fig. 1), (3) cutting through probable shrinkage cracks (Pl. 2, fig. 2), and (4) filling fissures along faults of possible syndepositional origin (Pl. 2, fig. 5).

Selenite crystals develop in apparently two ways: (1) downward movement of dense, hypersaline brines into sediment below with resulting formation of gypsum crystals (Masson [1955, p. 77] reported selenite of this origin forming in the mud flats of Laguna Madre, southwest Texas), and (2) evaporation of ground water in the vadose or capillary zone. Selenite crystals formed by this mechanism are indicators of subaerial exposure (Murray, 1964, p. 516, and Talmage and Wootton, 1937). Both mechanisms involve evaporation of water, either on the surface or in the subsurface, and are useful as environmental indicators.

Internal stratification has been totally destroyed in 14 units in which gypsum veins occur (Appendix 1). Several other units where gypsum veins are

PLATE 1

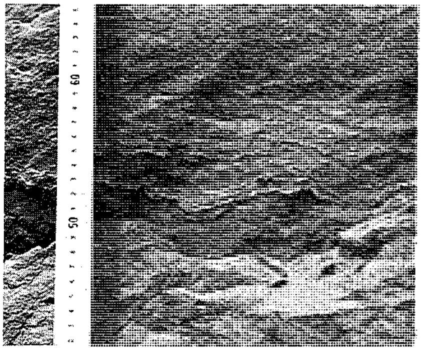
1

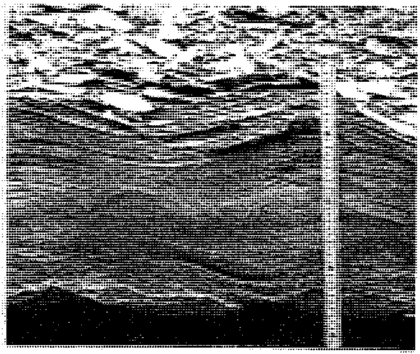
2

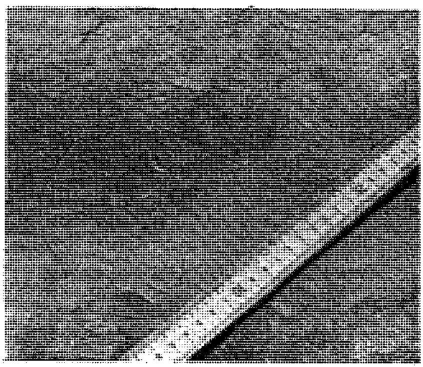
3

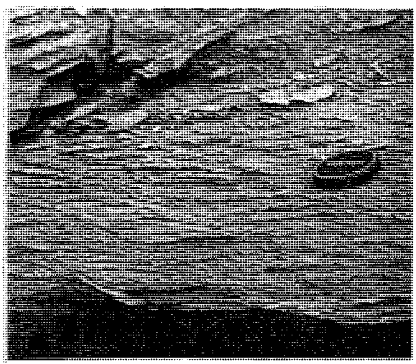
4

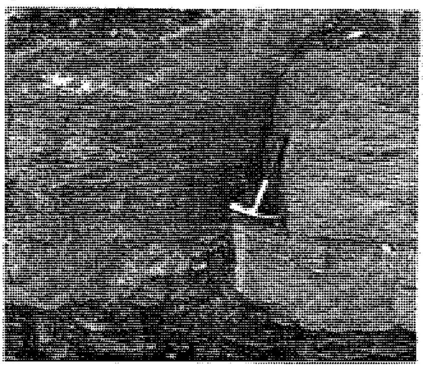
5

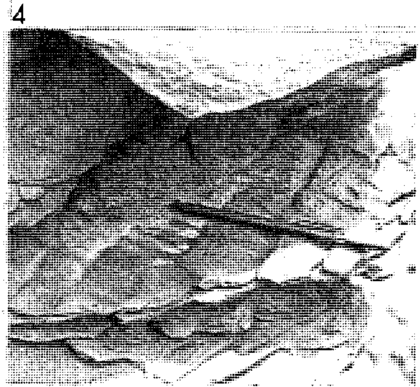
6

EXPLANATION OF PLATE 1
ENTRADA SEDIMENTARY STRUCTURES, CHERT AND GYPSUM

FIG. 1.—Deformed stringers of nodular chert, Entrada Sandstone.
FIG. 2.—Sinusoidal ripple-lamination, Entrada Sandstone, Unit 96.
FIG. 3.—Micro-cross-lamination, Entrada Sandstone, Unit 81.
FIG. 4.—Climbing-ripple lamination, Entrada Sandstone, Unit 71.
FIG. 5.—Gypsum veins, Entrada Sandstone, Unit 41.
FIG. 6.—Asymmetrical current ripple marks, Entrada Sandstone, Unit 85.

observed show evidence of deformed bedding, or soft-sediment deformation. Deformed stratification in these units may be related to, or primarily caused by, development or movement of gypsum.

Interpretation of the gypsum veins in the study area as being primary in origin eliminates one possible cause for deformed internal stratification, which is expansion resulting from the hydration of primary anhydrite and subsequent formation of gypsum. The separation of vein walls by directional crystal growth provides space for development of transverse gypsum veins (Bundy, 1956, p. 247). Such directional forces may also cause deformation of the enclosing sediment, particularly if the sediment is soft and the veins are numerous.

Silica Occurrence in Entrada Sediments

Red and white chert and gray megaquartz occur in the Entrada Sandstone studied. These silica minerals occur in irregular masses (stringers, blebs, and nodules), in siltstone and fine-grained sandstone, and in one instance as a continuous bed.

Chert and megaquartz occur together in the studied section in distorted stringers, either continuous for several tens of centimeters, or discontinuous (Pl. 1, fig. 1). Frequently, it appears that the silicious stringers conform to the disrupted attitude of the bedding of the sediments in which they occur. Isolated, B-B sized, nodular masses of red and white chert are also common (Pl. 4, fig. 3). Masses of chert up to 2 cm in diameter occur in Unit 70. Individual grains or blebs of chert, either red or gray, and commonly 2 mm in diameter are also found, as in Unit 79.

A distinct bed of white chert marks the contact between Entrada Units 70 and 71 and varies in thickness from 1 mm to 5 cm. It is continuous throughout the exposure where their contact is visible. Thin sections of this silicious bed show distorted, wavy threads and lenses of clay throughout the white chert. Silica occurs as microcrystalline non-fibrous quartz. Calcite and minor amounts of dolomite occur as void-filling and cementing minerals.

Irregular masses and stringers of silica in the Entrada Sandstone are considered to be syngenetic, penecontemporaneous with deposition, or syndiagenetic. Evidences suggesting such timing are the manner in which chert stringers are deformed, their obvious relation to the deformed stratification of the enclosing sediments, and their occurrence in fine-grained clastic rocks.

Origin of the chert bed in Unit 70 could be either syngenetic or replacement. Conclusive evidence is wanting. Folk and Pittman (1971) reported a method utilizing optical properties of chalcedony to indicate a replacement origin after evaporite minerals, but this method could not be applied here. Entrada chert is nonfibrous in nature and lacks pseudomorphs.

Several sources could have supplied the silica found in the Entrada Sandstone. A volcanic source—either subaerial weathering of contemporaneous volcanic rocks, or widespread air-borne volcanic material—is a possibility. The nearest volcanic activity during Late Jurassic time was a considerable distance to the west (Petersen, Rigby, and Hintze, 1973, p. 129); however, airborne ash from the west could be a source. Bissell (1959, p. 181) mentions the importance of biologic and organic agents as sources of silica in sediments, but evidence of those agents in the Entrada deposits is lacking. Streams carrying silica in solution from the weathering of silicious rocks of the provenance sur-

PLATE 2

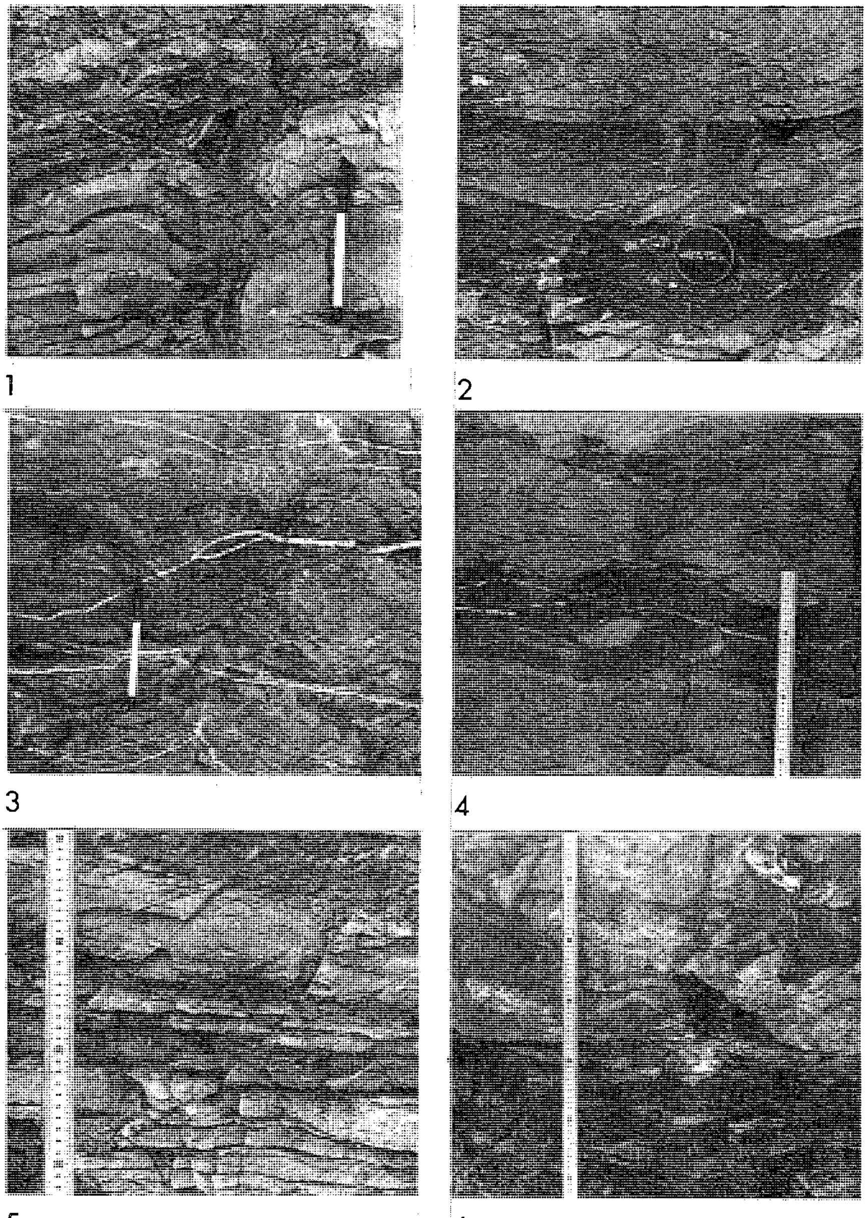

EXPLANATION OF PLATE 2

DEFORMATION STRUCTURES, ENTRADA SANDSTONE

FIG. 1.—Soft-sediment deformed, rotated block of sediment, Unit 49.
FIG. 2.—Shrinkage cracks in vertical section, Units 13 and 14.
FIG. 3. Tentlike loading structure, Unit 47.
FIG. 4.—Loading structures, Unit 38.
FIG. 5.—Small-scale, penecontemporaneous faults, Unit 44.
FIG. 6.—Loading structure, Unit 41.

rounding the Entrada depocenter could have supplied appreciable quantities of silica. Formation of jell-like masses of impure to pure silica have been reported in recent sediments in the Mississippi River Delta (Bissell, 1949, p. 177).

Sedimentary Structures

The sedimentary structures described are both syndepositional and postdepositional. Syndepositional sedimentary structures include ripple marks, cross-bedding, micro-cross-lamination, and climbing-ripple lamination. Postdepositional sedimentary structures include shrinkage cracks and rip-up clasts.

Ripple Marks.—Ripple marks are the result of the interaction of currents or waves on a noncohesive sediment surface. They are the most commonly observed sedimentary structure in the Entrada Sandstone, where they occur in most sandstone units and many siltstone units. Both current-produced and wave-generated ripple marks occur in the measured Entrada section.

Current ripple marks are the most abundant. They have regularly spaced, asymmetrical crests with wave lengths of 2 to 5 cm (Pl. 1, fig. 6). Crests are parallel and generally straight. Reineck and Singh (1973, p. 29) classify current ripples with wave lengths of normally less than 30 cm as small current ripples, and those with straight, parallel crests as straight-crested small ripples (Reineck and Singh, 1973, p. 30).

Ripple marks in the measured Entrada section interpreted as being produced by wave action are limited to Unit 96 and float blocks derived from the section between Units 27 and 33.

Ripple marks are identified as wave-generated ripples by symmetry, ripple indices and bifurcation of ripple crests (Tanner, 1967). Wave ripples are symmetrical, or slightly asymmetrical, normally straight crested, and frequently show bifurcation (Reineck and Singh, 1973, p. 24). Bifurcation, where a single ripple crest splits into two crests, is found almost exclusively in wind and wave-type ripple marks (Tanner, 1967, p. 101).

Tanner (1967), in a study of ripple indices, defined seven dimensionless parameters for determination of ripple mark geometry. Three of these parameters—ripple index, ripple symmetry index, and parallelism index—were utilized to aid identification of ripple genesis.

Cross-bedding.—Small-scale cross-bedding occurs throughout the Entrada section. Reineck and Singh (1973, p. 85) defined crossbeds with thicknesses of less than 5 cm as small-scale crossbeds. Cross-bedding in many instances is the result of migration of small ripples. Foreset laminae of a crossbed are the lee-side laminae of the ripples (Reineck and Singh, 1973, p. 85), and migration of small ripples produces small-ripple bedding. Small-ripple bedding results from low sediment availability and vigorous reworking.

Large-scale, trough-shaped cross-bedding occurs in Units 59 and 77. Unit 59 is a fine-grained sandstone and the upper part is composed of crossbed sets 50 cm thick. Unit 77 is a fine- to coarse-grained sandstone and is composed of 200 cm thick crossbed sets.

Micro-cross-lamination.—Micro-cross-lamination was described by Hamblin (1961) in his study of Upper Keweenawan sediments of Michigan. This structure is identical to trough cross-bedding "and is therefore significantly different from ordinary ripple lamination" (Hamblin, 1961, p. 390). Micro-

PLATE 3

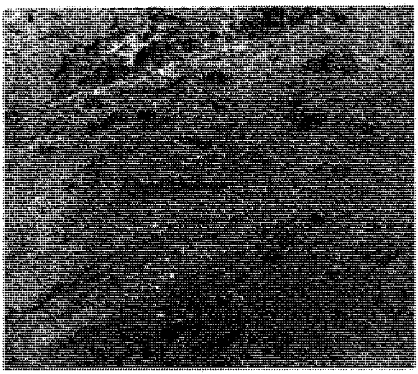

1

2

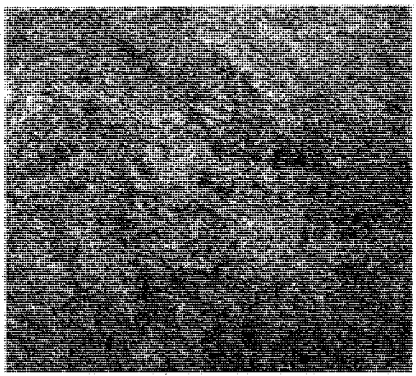

3

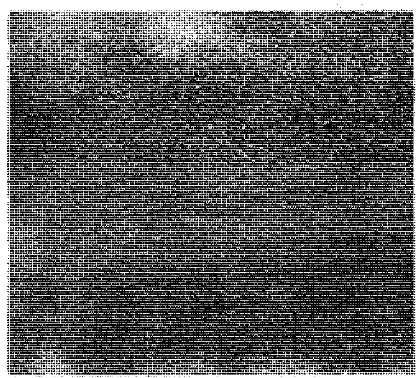

4

EXPLANATION OF PLATE 3

PHOTOMICROGRAPHS OF THIN SECTIONS

All photographs X5

FIG. 1.—Thin section of Unit 70, showing deformed nature of sediment.
FIG. 2.—Thin section of characteristic churned nature of Unit 80.
FIG. 3.—Thin section showing typical churned nature of Unit 95.
FIG. 4.—Thin section of Unit 50, lens "C," depositional interface of nonstratified siltstone with micro-cross-bedded siltstone.

cross-lamination is restricted in its occurrence to siltstone and fine-grained sandstone (Hamblin, 1961, p. 399). Such a restriction indicates a limitation on the range of energy levels within the depositional environment.

Ripple marks and mud cracks are normally associated with micro-cross-lamination. Because of this association, micro-cross-lamination in the Keweenawan sediments is considered to be the product of a shallow water environment that was repeatedly subjected to subaerial exposure and erosion (Hamblin, 1961, p. 399).

Micro-cross-lamination occurs in the Entrada Sandstone in fine-grained sandstone in Unit 81. The only expression of the structure is developed on a plan view (Pl. 1, fig. 3). The laminae form an arc which is concave in a down current direction. Individual sets of micro-cross-laminae are 4 to 5 cm wide and 19 cm long. This corresponds well with the average size of micro-cross-lamination sets described by Hamblin (1961, p. 392).

Paleocurrent directions measured on sets of micro-cross-laminations in the Entrada Sandstone are consistent, indicating current motion toward N 25° E. Paleocurrent trends obtained from current ripple marks exposed in the same unit are similar.

Sedimentary structures associated with micro-cross-lamination are small current ripple marks. Mud cracks are found only in the lower units of the Entrada, but were not seen where micro-cross-lamination was observed.

Climbing-ripple Lamination.—Climbing-ripple lamination, or ripple drift structures, are the internal structures formed in noncohesive sediment by migration and simultaneous upward growth of ripples produced by either currents or waves (Reineck and Singh, 1973, p. 95). The velocity of water and the sediment load cause distribution and genesis of climbing-ripple lamination. (McKee, 1966, p. D95).

The original ripple layers are preserved by currents causing formation and migration of ripples, rapid sediment influx, and concommitant burial of previously formed migrating ripples. A series of superposed ripples results which eventually produces climbing-ripple lamination (Reineck and Singh, 1973, p. 95). This sedimentary process involves sand acretion as well as migration.

Walker (1963, p. 176), in his study of ripple-drift cross-lamination, states that bed load movement alone would not cause the ripples to climb, and infers that the supply of sediment must come from suspension. McKee (1966, p. D98) also states that much of the sand must come from above by a settling of suspended load.

McKee (1965) describes two basic types of climbing-ripple lamination: ripple laminae in-phase, and ripple laminae in-drift. Jopling and Walker (1968) also describe two similar types of climbing-ripple lamination based on ripple morphology: type A where the stoss side is absent and only the lee side of the ripple is preserved, and sinusoidal ripple lamination, consisting of a series of ripples with symmetrical, sinewave profiles and continuous laminae across the ripple system. Jopling and Walker (1968, p. 983) interpret the change from type A to sinusoidal ripple lamination (in-drift to in-phase) as a result of a decrease in the ratio of the suspended load to the bed load.

Climbing-ripple lamination which occurs in the Entrada Sandstone is of both types: in-drift lamination, where only the lee side of the ripple is pre-

PLATE 5

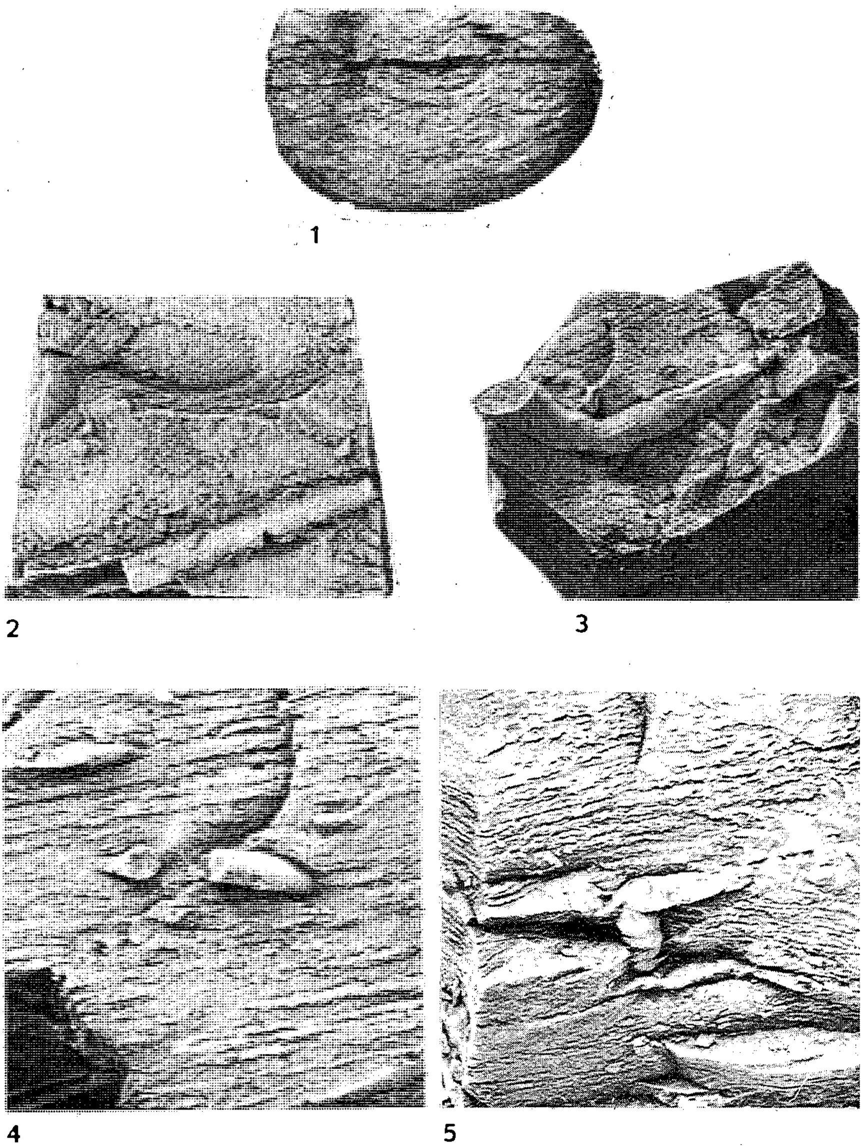

EXPLANATION OF PLATE 5

TRACE FOSSILS OF THE CURTIS FORMATION

FIG. 1.—U-shaped domichnid-type burrow, 2X.
FIG. 2.—Straight fodinichnid-type burrow, 2X.
FIG. 3.—Larger fodinichnid-type burrow, 2X.
FIG. 4.—Sinuous fodinichnid-type burrow, 2X.
FIG. 5.—Fodinichnid-type burrow showing lateral and vertical tubes, 2X.

served, and in-phase or sinusoidal, where both the lee and the stoss sides of the ripples are preserved.

Climbing ripples are readily observed in Entrada Units 45, 50, 57, 71, 81, 91, and 96. In-drift lamination, type 2 of McKee and type A of Jopling and Walker, occurs in Units 45, 50, 57, 71, and 81. Units 45 and 57 are fine-grained sandstone and climbing ripples are associated with normal small-scale ripple marks. Unit 50 displays several lenticular sandstone bodies where climbing ripples occur. Unit 71 is an interbedded series of rippled sandstone and mudstone, and climbing ripples occur in the sandstone. Here the ripple sets are 5 cm thick (Pl. 1, fig. 4) and are also associated with small-scale current ripples. Unit 81 is a silty sandstone and climbing ripples occur in sets up to 4 cm thick. In-phase ripple, or sinusoidal ripple lamination occur in Units 91 and 96. Small climbing ripples with wave lengths of 5 to 10 cm are observed in siltstone of Unit 91. Unit 96 is a sandstone and shows climbing-ripple lamination with wave lengths of 50 cm, and ripple troughs 5 cm deep with symmetrical, sinusoidal profiles (Pl. 1, fig. 2).

Climbing ripples occasionally form of net deposition from currents or waves, or in those environments where rapid accumulation of sediment takes place (Walker, 1963, p. 176). Jopling and Walker (1968, p. 971) describe climbing-ripple lamination as an important feature in fluvio-lacustrine deposits. McKee (1966, p. D96) found climbing-ripple lamination to be a common structure in flood plain and natural levee environments, but considered tidal flats and beaches as unlikely environments for its formation. Stanton (1975), however, in his study of the tidal flat sediments of the Summerville Formation, notes the occurrence of climbing-ripple marks. Reineck and Singh (1973, p. 97), following Wunderlich (1969), state that climbing ripples can be abundant locally at places of high rates of sedimentation.

Shrinkage Cracks.—Shrinkage cracks, or mud cracks, originate by dessication and compaction of water-saturated, cohesive sediments such as clay and silt, and in their typical development, form a surface network of irregular polygons (Shrock, 1948, p. 189).

Subaerial exposure of water-saturated sediment for extended periods is necessary for the development of shrinkage cracks.

In a transverse section shrinkage cracks occur as finlike or fingerlike extensions of the overlying deposit into the underlying sediments, and steep V-shaped profiles are typical (Reineck and Singh, 1973, p. 50). Entrada Units 13 and 14 display transverse sections of several shrinkage cracks (Pl. 2, fig. 2). They occur in the lower part of Unit 14, extend down through mudstone partings into a lower sandstone of that unit, and are filled with sediment typical of the sandstone directly above. These shrinkage cracks are 2 mm to 1 cm wide, steeply V-shaped, and 5 to 7 cm deep. Mud cracks in Unit 13 have a similar morphology to those in Unit 14, and appear to be filled with sand derived from the basal portion of Unit 14.

Rip-up Clasts.—Fragmented mudstone clasts incorporated in the base of a sandstone and derived from an underlying mudstone are termed rip-up clasts (Pl. 6, fig. 1). Evans (1965, p. 221) in his study of tidal flat sediments in the Wash, described scours, filled with mud flakes from tidal waters which stripped previously exposed and dessicated surface laminae. The mud flakes are usually small; however, Evans found larger fragments up to one foot

PLATE 6

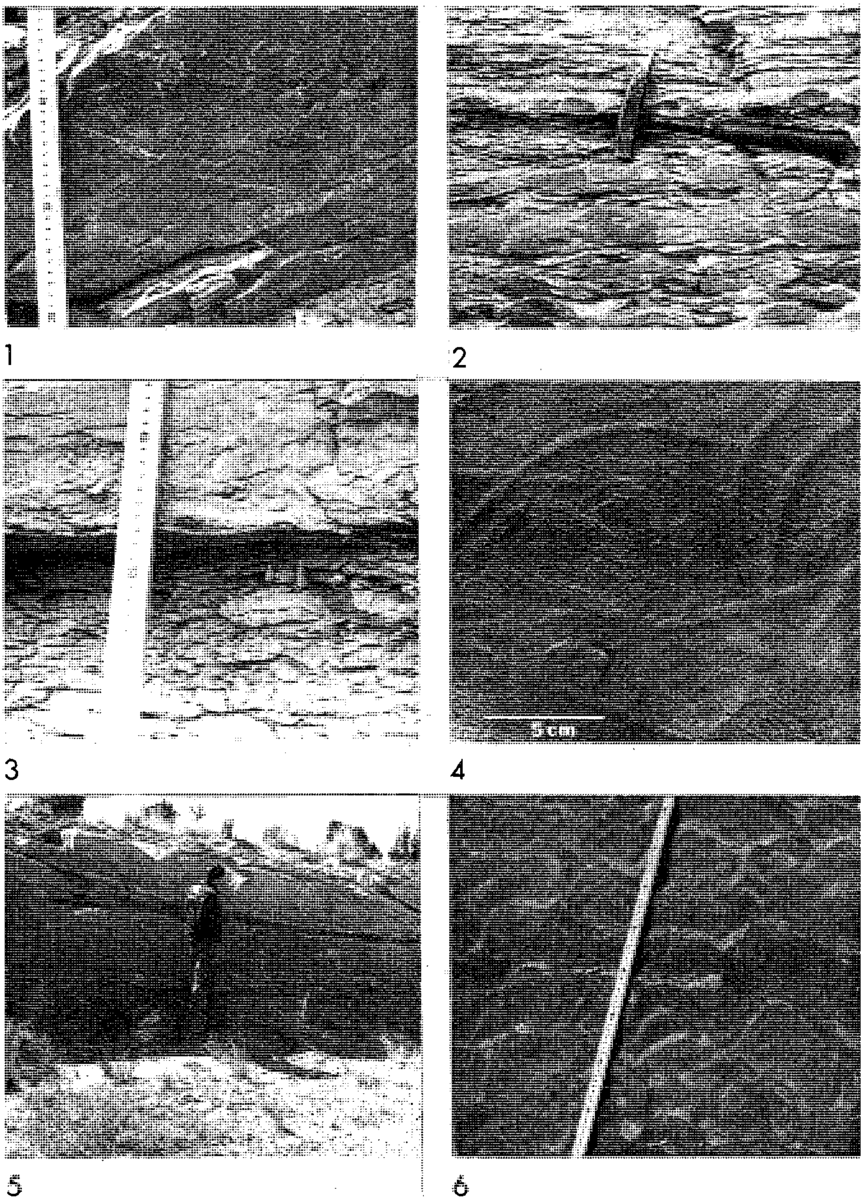

EXPLANATION OF PLATE 6

SEDIMENTARY STRUCTURES AND TRACE FOSSILS, CURTIS FORMATION

FIG. 1.—Rip-up clasts, Unit 8.

FIG. 2.—Rippled, lenticular nature of siltstone beds of the intercalated siltstone and claystone facies.

FIG. 3.—U-shaped domichnid-type burrow in claystone truncated at the top by siltstone bed, Unit 6.

FIG. 4.—Pascnichnid-type burrows, Unit 22, 0.5X.

FIG. 5.—Imbricate sandstone lenses of Unit 21.

FIG. 6.—Lingoid small ripple marks with superimposed small-current ripple marks, Unit 8.

square which were folded over and incorporated in the sediment. Shrock (1948, p. 257) labeled similar sedimentary structures as sharpstone conglomerate. He ascribed their genesis to mud crack-produced, polygonal, mud plates curling upward and pulling away from the underlying sand as dessication proceeds, and ultimately fusing into the base of the next deposit.

Rip-up clasts occur in the Entrada Sandstone in Units 19, 33, 38, 40 through 43, and 49. Rip-up clasts in Units 19, 40, and 42 are associated with channels or channel-fill sediments, and commonly occur at the base of channel-fill sandstones. The mud fragments are moderately rounded and some show considerable bending, indicating that the fragments were soft or semi-consolidated when ripped up by channeling currents. A few of the mud clasts are angular.

Rip-up clasts in Units 33, 38, 41, 43, and 49 occur in the basal portions of these sandstone units. Mudstones occur stratigraphically immediately below these sandstone units and are probably the parent material from which the rip-up clasts were derived.

Penecontemporaneous Deformation Structures

Deformed, distorted, and disturbed structures formed prior to consolidation and lithification of sediments by inorganic agents are termed penecontemporaneous deformation structures. These structures are generally localized, confined to a single bed between undeformed beds (Potter and Pettijohn, 1963, p. 143).

Penecontemporaneous deformation results from various processes. Slumping and sliding downslope results in deformation of sediments. Unequal loading or overloading by sediment may cause vertical as well as lateral displacement. Frictional drag by currents acting on previously deposited sediment can result in deformation structures (Potter and Pettijohn, 1963, p. 143).

Structures interpreted as penecontemporaneous deformation structures occurring in the Entrada Sandstone include load structures, faults, and distorted bedding.

Load Structures.—Load structures result from the deposition of sand on an unconsolidated or hydroplastic layer of mud. Soft sediments yield to differential loading primarily by vertical movement, whereby the sand sinks into the mud in the form of lobes, or where mud squeezes upward in finger-like projections (Reineck and Singh, 1973, p. 76).

Load structures occur in the Entrada Sandstone in several units and in several distinct shapes. Entrada load structures have one feature in common—all demonstrate injection of mud into overlying sand layers. The mechanism which caused the structures is most likely the same in all instances.

The basal part of Unit 38 displays an invasion of mud into sandstone in irregular, wavy tongues (Pl. 2, fig. 4). The load structure in Unit 41 has the form of a shark's dorsal fin (Pl. 2, fig. 6). Unit 47 displays a tentlike structure resulting from the vertical displacement of a mud lens within a sand body (Pl. 2, fig. 3).

Kuenen and Menard (1952, p. 90) in a study of turbidity currents, stated that one possible mechanism for structural deformation is "local settling and squeezing caused by rapid accumulation of overburden on the highly mobile foundation." The probable cause of load structures in the Entrada Sandstone is local upward squeezing of hydroplastic mud due to differential loading and rapid sedimentation of sand.

Small-scale Faulting.—Penecontemporaneous faulting is a widespread phenomenon in loose sand and silt and is commonly preserved in sedimentary rocks (Shrock, 1948, p. 259). Small-scale faulting was observed in two units, Units 10 and 44, of the Entrada Sandstone.

Broken, offset clasts of mudstone laminae occur across small faults in Unit 10 where the offset is about 1 cm. The dislocation dies out downward and is truncated above by deposition of a sandstone.

Thin layers of siltstone (1 to 2 cm thick) are offset by curved, concave upward faults in Unit 44 (Pl. 2, fig. 5). These faults do not affect the unit below, and they die out in a mudstone above. The faulting here is apparently postconsolidation or penecontemporaneous with consolidation, since the offset layers show no obvious flowage or other hydroplastic features.

Deformed Stratification.—Disruption and deformation of stratification within units of the measured section of the Entrada Sandstone are common, even in those units where gypsum does not occur (Text-fig. 2a-2d; Appendix 1). Deformation is manifested in the sediments by churned or contorted bedding or a structureless unit.

Much of the internal deformation may have resulted from bioturbation or rooting. Possible circular burrows were observed in Unit 1. Much of the disruption of stratification, however, is very subtle and typical bioturbation features or trace fossils are lacking. Thin sections of Units 70, 80, and 95 (Pl. 3, figs. 1, 2, and 3) show obviously disrupted sediment and perhaps bioturbated internal stratification. In these examples disruption of the bedding apparently occurred penecontemporaneous with deposition, while the sediment was soft and hydroplastic.

Two examples of deformation of apparently semiconsolidated sediment were observed in Units 38 and 49. Both show blocks of sediment seemingly torn up and rotated from their original sites of deposition, but still retaining angular forms with only slight distortion of stratification within them. The rotated block of sediment in Unit 38 is 45 cm long and 20 cm across, considerably larger than the block in Unit 49 which is less than 10 cm long (Pl. 2, fig. 1). Disruption of surrounding sediment is obvious in both examples. These blocks of sediment may have resulted from currents of water tearing up chunks of consolidated sediment during episodes of flooding, with little or no transportation of the blocks involved. Such an origin is similar to the formation of rip-up clasts, but on a larger scale and without channeling.

Lithologic Relations

Road cuts provide excellent exposures of the measured section of the Entrada Sandstone and clearly show sand bodies with lenticular shapes, channels and channel-filling sediments, and repeating mudstone and sandstone beds (Pl. 4, figs. 1, 2, and 4-7).

Numerous two-element cycles of red sandstone and mudstone characterize the lower fifty-five units and Units 64 through 68 of the studied section (Text-figs. 2a and 2b). This sedimentary pattern is interrupted by siltstone beds in only three places in the section. Sandstone units are generally thicker than mudstone units, more resistant, and form rather prominent ledges, while mudstone units are thin and recessive. Units of both lithologic types are uniform and laterally continuous. Boundaries between units are sharp and well defined.

The sandstone-mudstone cyclic depositional pattern suggests a repetition of a set of environmental conditions. This repetition of a set or sets of conditions was most likely a simple cyclic occurrence without any regularity of period, rather than rhythmic deposition, implying deposition at regular or regularly varying periods of time.

Cyclic deposition observed in the measured section perhaps results from cyclic changes of water depth, or activity of intermittent floods or storms. McCrone (1964, p. 278), in a review of water depth and cyclothem deposition, related several depth-related environmental factors including (1) desiccation cracks and crack fillings, (2) sharp contacts of successive rock layers that are thin, widespread, and uniform, and (3) uniform thicknesses of several beds in a given succession, all separated by sharp boundaries. McCrone explained that sedimentary structures such as these result from repeated and sudden depth changes. Intermittent flooding or storm activity could contribute to the formation of a cyclic sedimentary pattern such as occurs in the studied section.

Channeling and channel-filling sediments of two types occur in the measured section and are (1) a sandstone-filled channel cut into mudstone, and (2) mudstone-sandstone filled channels cut into a thick sandstone unit. Both types of channels are associated only with cyclic sandstone and mudstone deposits.

Unit 19, a prominent 140 cm thick sandstone, occurs channelling into thin mudstone and sandstone beds of Units 17 and 18. The unit thickens to 180 cm where it truncates and channels out the lower units. Here it forms a channel 40 cm deep, rather steep-walled, flat bottomed, and broadly U-shaped. In basal parts of the channel numerous mudstone rip-up clasts occur (Pl. 4, fig. 5). Channeling by sand of Unit 19 was apparently localized and was observed only in one place along the entire 150 meter length of the easternmost road cut.

Unit 41 is a prominent ledge-forming sandstone cut by a series of three sediment-filled, concave upward lenses. Geometries and internal structures of these lenses suggest that they be interpreted as channels. For channel location and designation refer to Plate 4.

Channel A is shallow, less than 25 cm deep, and its internal morphology was difficult to ascertain. Channel B occurs 75 cm west of Channel A and is 75 cm deep. Sediments filling Channel B (Pl. 4, fig. 1) consist of alternating thin beds of red mudstone and green sandstone. These alternating layers are symmetrical and conform to the shape of the channel with concavity upward, and tend to thin out laterally on the sides. McKee (1957, p. 133) stated that channels with similar internal geometries result from deposition by longitudinal currents in completely submerged channels.

Channel C occurs 250 cm west of Channel B and is 75 cm deep. Channel C has a 30 cm thick basal sandstone, which is strongly asymmetrical, ripple marked, and contains numerous rounded and a few angular mudstone rip-up clasts (Pl. 4, fig. 2). The basal sandstone is overlain by a series of concave upward, symmetrical, thin beds of red mudstone and green sandstone similar to those in Channel B. According to McKee (1957, p. 133) deposition of asymmetrical channel filling results from a submarine current passing diagonally over the channel. Reineck and Singh (1973, p. 63) state that diagonal filling of channels is commonly observed in tidal zones when intertidal flats are still under water, and flow of water is controlled by difference in water levels rather than by surface morphology.

Lenticular sandstone bodies occur in the measured section both with a flat bottom, convex-upward geometry and a biconvex geometry. These sandstone lenses are associated with cyclicly deposited sandstone and mudstone beds and occur in Units 43 and 50.

The prominent sandstone lens in Unit 43 has a flat bottomed, convex-upward shape (Pl. 4, fig. 4). The lens attains a maximum thickness of 50 cm, and a width of approximately 4 meters. Field relations suggest that this lens, and perhaps others adjacent to it, acted as a barrier to sediments being transported in an easterly direction, normal to the strike of the barrier. Apparently, the energy of the transporting medium, water, was insufficient to breach or overtop the barrier with sand; thus, deposition of sand occurred on the up-current side of the barrier, while finer clastic particles were carried in suspension over the barrier and deposited on the down-current side. Field relations further suggest rapid burial of this barrier, perhaps in a single event such as a storm.

Three wide, low-profile sandstone lenses, designated A, B, and C on Plate 4, occur in Unit 50. A prominent recessive unit, Unit 50 is an interbedded sequence of thin mudstone and sandstone beds with the three lenses being the most conspicuous structures of the Unit.

Lens A is approximately 14 meters wide and 60 cm thick at its midpoint. Geometrically, Lens A is convex-upward with a flat bottom, similar to the smaller lens in Unit 43. The lens was inaccessible for detailed examination and no internal structures were noted. Overlying beds of thin mudstone and sandstone deform and bend over the upper surface of Lens A, while a mudstone bed either thins beneath the lens or was truncated when deposition of the lens took place.

Lens B occurs immediately west of Lens A and overlaps the western edge of Lens A. Lens B is 15 meters wide, attains a maximum thickness of 60 cm, and displays a biconvex shape. There is no apparent truncation of beds underlying this lens, and those beds which overlie the lens deform and bend over the upper surface. Lenses A and B, occurring at about the same stratigraphic interval, represent penecontemporaneous deposition.

Lens C, stratigraphically below Lenses A and B, is 12 meters wide, a maximum of 50 cm thick, and has a biconvex geometry. Beds both above and below this lens are deformed and bend around the lens. Lens C is a very fine-grained sandstone with cross-bedding common in the basal part, and climbing-ripple lamination also evident. Micro-cross-bedding was observed in a thin section from a sample of the lens (Pl. 3, fig. 4).

Lawyer (1972, p. 116) interpreted a flat-bottomed, convex-upward lens of sandstone in the Dakota Sandstone as a splay (crevasse deposit) in a flood-plain environment.

Deposition of sand in soft, unconsolidated mud results in differential compaction of the sediment beneath the sand, causing deformation and subsidence of the sand body, so that the present cross-sectional shape is not necessarily the original one (Pettijohn, Potter, and Siever, 1973, p. 442). The relationship of these lenses to the enclosing sediment suggests depositional rather than erosional boundaries and thinning of mudstone layers beneath the lenses indicates subsidence and differential compaction.

Interpretation of the Sedimentary Environments of the Entrada Sandstone

Sediments of the studied section of the Entrada Sandstone are interpreted to represent deposition in four distinct sedimentary subenvironments within a complex interdeltaic-coastal system. This complex depositional system existed on the margin of a broad, shallow, regressive epicontinental sea. The hypothetical Late Jurassic 25° north latitude (Text-fig. 3) was positioned approximately 3° south of the Entrada depocenter (Tanner, 1965, p. 572), and therefore the climate was most likely warm and semiarid.

These four interdeltaic depositional subenvironments were apparently products of low-energy, nearshore processes and produced (1) cyclic sandstone and mudstone deposits, (2) thick sandstone and siltstone deposits, now characterized by "stone baby" weathering habit, (3) large-scale, cross-bedded sandstone deposits, and (4) thin, green sandstone deposits. Each of these types of deposits represents a specific subenvironment which may be recognized by its lithology or sequence of lithologies, characteristic sedimentary structures, and mineral associations. Probable sedimentary processes active during deposition of these environments were (1) current and wave action, (2) tidal processes, (3) storm activity, (4) deltaic processes, and (5) biologic processes. Text-figure 4 shows graphically in vertical section the succession of the four subenvironments as they occur in the measured section.

The sediments of the subenvironment represented by cyclic sandstone and mudstone deposits occur in Units 2 through 55 and Units 64 through 68, and occupy 35 meters of the total 125 meters of the section. These units are characterized by channels, small-current ripple marks, possible wave-generated ripple marks, climbing-ripple lamination, penecontemporaneous deformation features such as load structures and deformed bedding. Shrinkage cracks, lenticular sandstone bodies, and numerous gypsum veins also occur, as well as a single incidence of selenite.

Ripple structures show a dominant east-northeast current trend, except in Units 7 and 8, where northeast-southwest bimodal current directions are evident (Text-figs. 2a and 2b). The unimodal paleocurrent trend perhaps indicates the direction from which the sediments of this environment were derived and the processes involved in their transportation. Most of the sediments deposited in an interdeltaic system are continentally derived. Sediment carried to the shoreline by rivers and streams is dispersed laterally by marine currents for great distances along the coast. Clay and fine silt are carried in suspension while sand is transported mainly as bed load or by wave action in the nearshore zone (LeBlanc, 1972, p. 163). Bimodal current directions indicate perhaps tidal influences within the depositional environment.

The red color of the beds, caused by oxidation of the iron content of the sediment, the shrinkage cracks, and the occurrence of selenite strongly suggest limited subaerial exposure of the sediments of this environment.

Climbing-ripple lamination (Units 45 and 50) and load structures (Pl. 2, figs. 4 and 6) are indicative of local rapid deposition of sand. Postulated burial of a small lenticular sand barrier (Unit 43) also suggests periods when

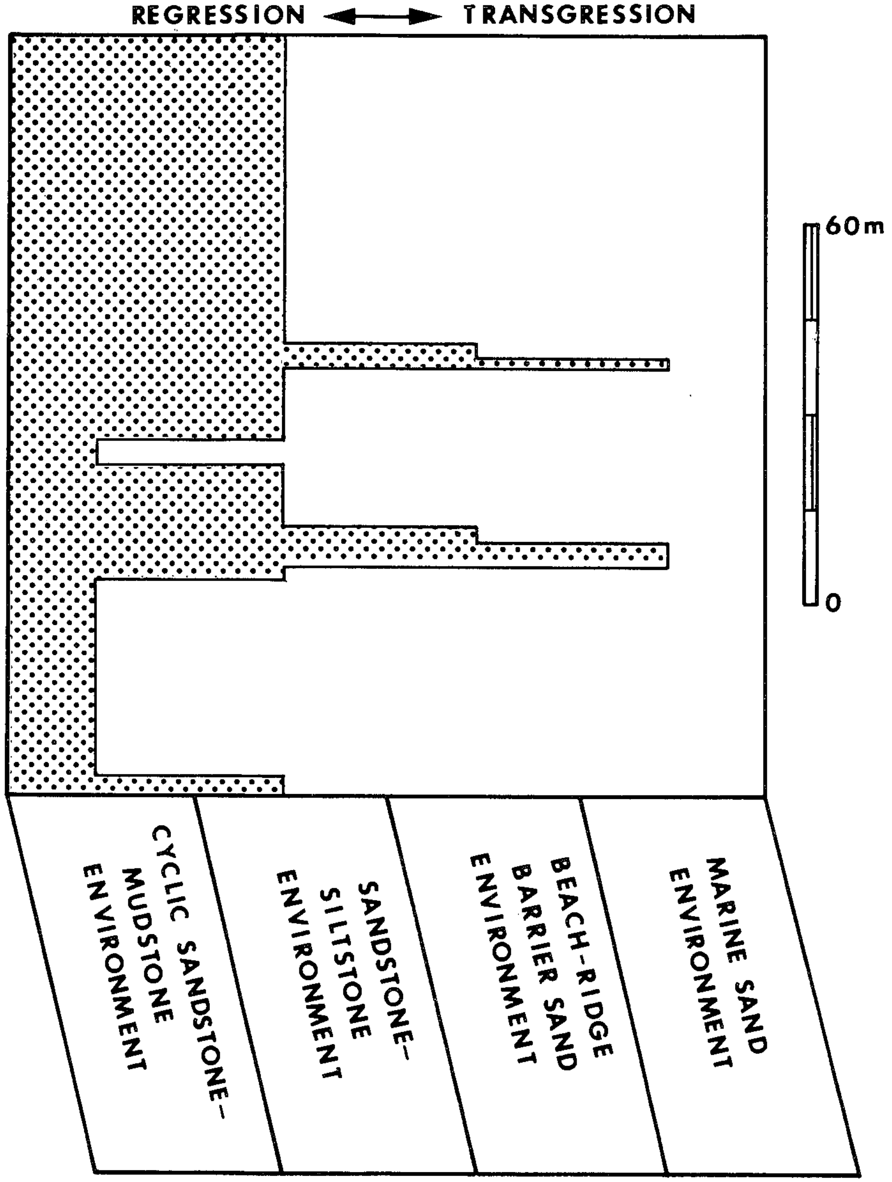

TEXT-FIGURE 4.—Graphic representation of the repetitive occurrence of the four different sedimentary environments of the Entrada Sandstone in vertical section, showing transgressive and regressive phases and thickness of the section representing each environment.

depositional rates were accelerated. Intermittent storms could produce currents with energy levels capable of transporting quantities of sand in suspension, thus creating such sedimentary structures.

Channels are restricted to the cyclic sandstone and mudstone depositional environment and occur in Units 19 and 41 of the measured section. Rip-up clasts in the basal part of the channel in Unit 19 indicate that sand was deposited on soft, unconsolidated mud. The series of three channels in Unit 41 may be either tidal or fluvial in origin. Sediments filling the channels suggest, however, deposition in completely submerged channels, which would be more representative of tidal zones.

Possible deltaic processes of small rivers are suggested by the series of sandstone lenses in Unit 50. These lenses are depositional structures, and may be splay deposits created by crevassing through the natural levees of small rivers. Climbing-ripple lamination occurs in one of the lenses and suggests rapid deposition, a process which would be expected in crevasse splay deposits. Substantiating evidence for fluvial deposition is lacking, however.

Biologic processes such as bioturbation and rooting may account for the churned, deformed nature of the internal stratification of many of the sandstone beds deposited in this environment. Organic activity is common in sandstone bodies of an interdeltaic system such as cheniers and barrier bars.

Typical sedimentary structures and vertical sequence of sediments indicative of a specific subenvironment within the interdeltaic depositional system as defined by LeBlanc (1972) are not evident in the measured section. Therefore, classification of the cyclic sandstone and mudstone facies as being representative of one or more of the six distinct types of deposits listed by LeBlanc (1972, p. 165) mud flat, chenier, barrier island, lagoon, tidal channel, and tidal delta is not possible. The environment suggested by the sedimentary structures and vertical sequence of sediments of the measured section reflects both tidal and perhaps fluvial processes, with tidal processes being dominant. It was an environment where subaerial exposure occurred as well as inundation by water highly charged with sand capable of eroding channels or burying previously deposited sand barriers. Sediments of this environment reflect possible frequent storm activity and perhaps flooding.

Sediments representing the thick sandstone and siltstone subenvironment occur in Units 1, 56, 60 through 63, 69 through 73, and Units 78 through 97 and occupy 82 meters of the total 125 meters, or three-fourths, of the measured section. This same facies comprises the lower 45 meters of the Entrada Sandstone not included in this study.

Sediments of this environment are characterized by irregular masses and stringers of red and white nodular chert (Pl. 4, fig. 3), deformed, churned stratification, climbing-ripple lamination, small-current ripple marks, micro-cross-lamination, irregular lenses of coarser sand, and limited mudstone deposits.

Paleocurrent trends indicated by directional structures in sediments of this environment show dominant current motion toward the northeast, with a minor component toward the west-northwest (Text-figs. 2b-2d). No mutually opposed bimodal current modes were observed. This paleocurrent trend indicates current motion and sediment dispersal approximately paralleled the postulated Late Jurassic paleoshoreline (Text-fig. 3).

A probable shallow water environment with local centers or periods of rapid sand accumulation is indicated by the occurrence of micro-cross-lamination and climbing-ripple lamination.

Chert, where it occurs in the measured section, is interpreted to be syngenetic in origin. Environmental implications of chert in sediments of this environment are difficult to interpret. Chert perhaps indicates precipitation of silica where fresh waters and marine waters interface, or it could indicate airborne volcanic material carried into the depocenter.

Deformed, churned internal stratification typifies much of the sediment of this environment. This stratification probably reflects organic processes such as bioturbation and rooting.

Classification of this particular sedimentary environment utilizing diagnostic sedimentary structures and vertical sequence of sediments and relating them to a known depositional environment with modern analogues has not been accomplished. Modern analogues of this environment and the previously described environment either have not been studied and described or do not exist.

This thick sandstone and siltstone facies was deposited primarily in shallow water in an environment where finer terigenous clastic material was either not available to be deposited, or bypassed the depocenter. That it was an oxidizing environment, perhaps subaerially exposed for intermittent periods, is reflected in the red color of the sediment. Biologic processes were apparently active. Lateral relationships of the thick sandstone and siltstone facies with the cyclic sandstone and mudstone facies are not readily apparent, but the vertical sequence (Text-fig. 4) suggests that the sand and silt accumulation was most likely situated seaward where current activity would limit deposition of muds.

The third subenvironment within this Late Jurassic coastal-interdeltaic depositional system is represented by sediments of two units, Units 59 and 77. These units consist of large-scale, cross-bedded sandstone. Paleocurrent directions indicated by dip direction of crossbeds in Unit 59 show current motion toward the west, while the dominant paleocurrent trend of cross-bedding in Unit 77 is toward the southwest. Paleocurrent trends such as these indicate off-shore directed currents, or seaward dipping cross-stratification.

These two sandstone units may have originated from either water current processes or eolian processes. Because of grain size and grain relationships, particularly in Unit 77, and the sequence of bedding in Unit 59, these sandstones are most likely products of water current processes. Unit 77 displays graded bedding of its foreset laminae, with very coarse sand defining the lower bounding surface of each foreset. The unit is generally poorly sorted. Unit 59 is horizontally laminated in the lower 100 cm and cross-bedded only in the upper 50 cm.

These cross-bedded sandstones are interpreted as low-profile beach ridges or barriers of some type. In vertical section, both are associated with thin green sandstone below and thick sandstone and siltstone deposits above (Text-fig. 4).

The fourth distinct environment within this depositional system is represented by sediments of Units 58 and 75, thin, light, olive gray sandstones. The color of these sediments indicates reduction of iron such as occurs in subaqueous conditions. These units are ripple marked and cross-laminated and probably resulted from deposition during short-lived, rapid marine transgressions. Both of these deposits are overlain by sediments interpreted as beach ridges or barrier sandstones (Text-fig. 4).

CURTIS FORMATION

The Curtis Formation unconformably overlies the Entrada Sandstone in the study locality. Here the Curtis section is approximately 65 meters thick, and most of the rocks observed are grayish olive colored, setting them apart from the red beds of the Entrada Sandstone below, and the red beds of the Summerville Formation above.

Lithologies of the Curtis Formation

Only terrigenous clastic rocks are found in the studied section of the Curtis Formation. Conglomerate, sandstone, siltstone, or claystone comprise the twenty-six units described (Text-figs. 2d and 2e; Appendix 2). From the base up, the gross vertical sequence is conglomerate, interbedded siltstone and claystone, sandstone, and interbedded siltstone and sandstone.

Conglomerate.—Conglomerate occurs in Units 1 and 7 of the Curtis section. The basal conglomerate, Unit 1, marks the unconformable contact of the Curtis Formation on the underlying Entrada Sandstone. Unit 1 is a light olive gray, poorly sorted, friable, pebble conglomerate and its thickness varies from 5 to 10 cm. Clasts vary greatly in size, with diameters ranging from 2 mm up to 6 cm. Clasts are composed of quartzite, limestone, chert, and clay and occur as broken and unbroken rounded pebbles and flattened pebbles with no preferred orientation. A fine-grained, poorly sorted, calcite-cemented matrix of quartz, feldspar, glauconite, and clay minerals supports the clasts. An appreciable percentage of the quartz grains in the matrix are well rounded with frosted surfaces.

Unit 7 is a calcite-cemented, poorly sorted, clay-pebble conglomerate, and its occurrence marks the termination of clay deposition here during Curtis time. Sandstone is the dominant lithology stratigraphically above Unit 7. Clasts in Unit 7 are composed of reworked material derived from the clay and silt upon which Unit 7 was deposited. Clasts with diameters of 10 cm were observed in the studied section. Fragments of macerated woody (?) organic matter are abundant. The matrix of Unit 7 is moderately sorted and composed primarily of angular to rounded, very fine sand-sized, quartz grains and minor amounts of glauconite, feldspar, and pyrite.

Claystone.—Claystone comprises 80 percent of the total thickness of Units 2 through 6 and all of Unit 25 of the measured section of the Curtis Formation (Text-figs. 2d and 2e; Appendix 2). The claystone in Units 2 through 6 is grayish olive colored on weathered surfaces and grayish olive green on fresh surfaces. Bedding is horizontal, finely laminated and discontinuous. Locally, the claystone is intensely rippled and cross-laminated on a small scale. Stringers of secondary gypsum are numerous and are generally concordant with bedding. Carbonaceous matter is abundant throughout these claystone units. Organic fragments up to 3 mm long are commonly observed on parting surfaces. Crossbeds tend to be accentuated as a result of deposition of clay-size carbonaceous fragments. Pyrite occurs in Unit 2 as silt-sized cubes disseminated among the organic fragments. Clay minerals make up 90 percent of the rock, with organic fragments, quartz, and mica composing the remaining 10 percent. Intense reaction of the claystone to dilute hydrochloric acid indicates abundant calcite cement. Domichnid and fodinichnid trace fossils were collected from Units 2, 4, and 5.

Claystone in Unit 25 is grayish red and grayish olive, 10 cm thick, slightly calcareous with numerous organic fragments occurring within the unit. No trace fossils were observed in Unit 25.

Siltstone.—Siltstone occurs in Units 2 through 6 and in Units 23 and 24 of the Curtis section. In Units 2 through 6, it occurs in yellowish gray, resistant units which are repetitively interbedded with claystone (Text-fig. 2d; Appendix 2). Siltstone beds in Units 2 through 6 vary in thickness from 1 to 25 cm and stand out in relief from the more recessive grayish olive claystone. Many siltstone beds thicken and thin, but are continuous along strike. Some however, are discontinuous and lenticular. Siltstone lenses vary in length from several centimeters to several meters. Small-scale crossbeds and rippled surfaces characterize the siltstones (Pl. 6, fig. 2), and some crossbeds indicate bimodal current directions. Quartz comprises 70 percent of the siltstone. Potassium feldspar (20 percent), plagioclase (5 percent), muscovite and organic fragments (5 percent) are also present. Quartz and feldspar grains are angular to subrounded. Siltstone in these units is highly calcareous and effervesces strongly with dilute hydrochloric acid. No fossils were recovered from the siltstones.

Siltstone in Unit 23 is argillaceous, quartzitic, with about 10 percent glauconite. It is grayish olive, laminar bedded, with angular detrital grains. Unit 23 forms a low-angle slope.

Siltstone in Unit 24 is grayish olive and composed of medium silt-sized grains which are well sorted. The grains are mostly quartz, angular to subrounded, with a small percentage of angular feldspar and rounded glauconite. The bedding is laminar. Numerous lenses of gray clay occur in a 2 cm thick zone in the middle of the unit. These clay lenses are parallel to the bedding and express a definite linearity. The lensses are up to 1 cm long and 2 mm thick.

Sandstone.—Sandstone is the dominant lithology found in the measured section of the Curtis Formation and occurs in Units 8 through 23 and Unit 26 (Text-figs. 2d and 2e; Appendix 2). Sandstone varies from light olive gray to greenish gray to dusky yellow to pale brown. Color varies from unit to unit and within some units. Modal composition of the sandstone deviates slightly from unit to unit with quartz being the dominant component (65 to 75 percent). Potassium feldspar (10 to 20 percent), plagioclase (0 to 10 percent), glauconite (2 to 10 percent), and pyrite (0 to 3 percent) constitute the remainder. Carbonaceous fragments are abundant and all sandstone units are dolomite cemented. Size sorting of the grains is moderate throughout the units while grain rounding varies from angular to subrounded. Units 8, 11, 12, 13, 15 to 23, and Unit 26 are very fine-grained sandstone, while Unit 14 is fine-grained sandstone.

Current ripple marks, megaripple marks, micro-cross-lamination, and trough-shaped crossbeds were observed at various locations throughout the Curtis sandstone interval except in Unit 18, which is finely laminated. Ripple marks vary in size with a maximum wave length of 13 cm and a maximum height of 2 cm as seen in Unit 10. Megaripple marks in Unit 14 attain maximum heights of 50 cm, and wave lengths of 8 meters. Individual crossbeds attain maximum heights of 20 cm, as those in Unit 14. Carbonaceous fragments are particularly abundant in ripple and megaripple troughs and on cross-bed foresets.

Pascnichnid-type burrows occurring in Unit 22 are the only evidence of trace fossils in the sandstone facies. No body fossils were observed.

Trace Fossils of the Curtis Formation

The only fossils found in the studied section of the Curtis Formation are ichnofossils (trace fossils) occurring in the lower claystone units and in the sandstone of Unit 22. Four distinct types of ichnofossils were observed there. Classification is based on a nomenclature proposed by Seilacher (1964) and trace fossils in the Curtis Formation include dwelling burrows (domichnia), feeding burrows (fodinichnia), and winding "grazing" burrows (pascnichnia).

Domichnid-type burrows are full-relief, U-shaped, and are consistently nearly perpendicular to the bedding. They occur in the upper part of the laminated claystone of Unit 6 but are sharply truncated by a resistant siltstone bed within the unit (Pl. 6, fig. 3). These domichnid burrows (Pl. 5, fig. 1) are similar to *Corophioides* (Hantzschel, 1962, p. W189). Limbs of the burrows are not parallel but converge upward so that the entire burrow resembles a miniature horseshoe. Maximum distance between the limbs is 10 mm at the bottom of the burrow, and 5 mm at the top. The diameter of each tube is 5 mm. Fillings of these burrows are more coarse grained than the sediment in which they occur.

Fodinichnid-type burrows in the Curtis Formation are smooth, nonornamented, and full-relief forms. Their courses are straight (Pl. 5, fig. 2) or slightly sinuous (Pl. 5, fig. 4) with a simple branching system. These burrows occur parallel to bedding surfaces, with branches that extend both laterally and vertically into adjacent sediment (Pl. 5, fig. 5). In cross section, the burrows are both circular and eliptical, with diameters ranging from 2 to 3 mm. Burrow segments up to 4 cm long have been obesrved.

Fodinichnid-type burrows 5 to 7 mm in diameter occur contemporaneously with the smaller diameter burrows. These larger burrows are full-relief, nonornamented, with eliptical cross sections, and with curved courses but often cross bedding planes (Pl. 5, fig. 3).

Pascnichnid-type burrows occur in sandstone in Unit 22. These burrows are convex-epirelief forms which are horizontal, and curved but not meandering (Pl. 6, fig. 4). Simple branching occurs in some of the burrows, while a rather complex but random crossing system involves most of the burrows. Diameters of pascnichnid burrows range up to 5 mm.

Glauconite

Glauconite occurs in the Curtis Formation in feldspathic sandstone, Units 8 through 23, and in the conglomerate, Units 1 and 7. Its abundance in these units varies from less than 2 percent (Unit 7) to 10 percent (Units 9 and 23). Glauconite occurs in the sandstone units and in Unit 7 conglomerate as very fine sand-sized (0.125 to 1.077 mm in diameter) grains, and in the basal conglomerate (Unit 1) as medium sand-sized grains (0.5 to 0.25 mm in diameter).

Glauconite may be authigenic or detrital. Utilizing the criteria determined by Light (1952), primarily grain surface structures such as lobate, grooved, or tabular surface indentations, or the absence of such characteristics, or grain shapes such as irregular, broken, and fragmental, the mode of occurrence of glauconite can be resolved. Glauconite grains in Units 8 through 23 are subrounded to rounded, and display distinctive subspherical, polylobate, and ovaloid surface structural shapes. They appear to be authigenic. Glauconite in Unit 1 occurs in the matrix of the conglomerate and the grains are dark green, smooth surfaced with no systematic surface structures, and nonrounded and irregular in shape. Glauconite here appears to be detrital. Glauconite grains in Unit 7 are rounded with some having remnants of former surface structures, and some having more well-defined surface indentations. Individual grain surfaces are either smooth, as in detrital grains, or rough and pitted, as occur in authigenic grains (Light, 1952, p. 74). Glauconite in Unit 7 is probably authigenic, but no particular grain characteristic occurs consistently, making Light's criteria nondiagnostic in this instance.

Dolomite Occurrence in the Curtis Formation

Dolomite occurs as the primary cementing agent in all sandstone units of the Curtis Formation. It appears that the dolomite developed as a replacement for calcite cement is sandstone operating within Curtis sediments early in the diagenetic process.

In recent restricted supratidal sediments (Deffeys, Lucia, and Weyl, 1965), evaporation of sea water produces magnesium-rich, hypersaline, high density brines. Under pressure of hydrostatic head, these brines percolate downward through permeable sediments, replacing calcium with magnesium. The calcite recrystallizes as dolomite. This process is dolomitization by seepage refluxion (Adams and Rhodes, 1960).

The seepage refluxion model of Adams and Rhodes (1960) treated the problem of dolomitization of extensive beds of limestone. This model requires a lagoon with a reef barrier to prevent free circulation of waters from the lagoon and thereby concentrating the brines. Deffeyes, Lucia, and Weyl (1965), proposed reflux dolomitization developed within a supratidal environment, with hypersaline brines being produced by continually evaporating sea waters and subsequent precipitation of calcium carbonate and gypsum.

Geologic environments of extensive reefs and lagoons required by the Adams and Rhodes reflux model were not produced during deposition of Curtis sediments. The Curtis Formation does not contain sediments produced in a subaerial supratidal environment. Laterally, the Curtis Formation changes facies to the east of the study area and there its equivalent is the Summerville Formation (Baker, Dane, and Reeside, 1936, p. 47). In the study area, overlying the marine Curtis deposits, are the tidal flat sediments of the Summerville Formation (Stanton, 1975). Hypersaline brines were produced on extensive supratidal mud flats shoreward from the depocenter of Curtis-type sediments. These brines probably moved downward through permeable channels, seeped into the Curtis sand, replaced calcium with magnesium, and produced a dolomite cement.

Sedimentary Processes and Paleoenvironments of the Curtis Formation

Conglomerate Facies.—Conglomerate of Curtis Unit 1 occurs as a thin basal deposit at the contact with the underlying Entrada Sandstone. The basal conglomerate reflects a transgression of the Curtis Sea during Oxfordian time over an emergent, possibly fluvially dominated landscape in the study area. Fine-grained sediments of the Entrada interdeltaic depositional environments observed in the Entrada section were apparently succeeded by coarse-textured fluvial sediments. The basal Curtis conglomerate possibly represents a lag deposit produced during the initial transgressive phase.

Clay-pebble conglomerate occurs at the interface of the interstratified siltstone and claystone facies with the overlying sandstone facies. The conglomerate is stratigraphically restricted and localized in the vicinity of the Interstate road cut. No evidence of similar sediments was observed in adjacent Curtis exposures. The localized clay-pebble conglomerate is probably a result of geographically restricted, temporary, high-energy currents. Semiconsolidated lumps of clay were most likely picked up from the underlying clay beds by these high-energy currents, transported and shaped in the aqueous medium, and deposited a relatively short distance from their points of origin.

Intercalated Siltstone and Claystone Facies.—The intercalated siltstone and claystone facies represents initial fine-grained clastic deposition in the study area. These fine-textured clastic rocks are transgressive deposits and are characterized by a series of upward-fining, claystone up to siltstone cycles in which claystone beds are repetitively interrupted by thin beds of siltstone. The fine-grained texture of the claystone is most likely the result of slow, nearly continuous deposition. Fine grain size may also be a reflection of paleotectonic control. Brenner and Davies (1974, p. 407) surmised that positive areas adjacent to the Oxfordian seaway were initially low lying and account for the muddy nature of early transgressive deposits.

The coarser interbeds of siltstone in this facies are probably the result of short-lived, high-energy currents. Such currents, possibly storm generated, could have introduced the coarse sediment fraction into the depocenter. Evidence of such a pattern is the highly rippled, cross-bedded, and lenticular nature of the siltstone interbeds, and the termination of U-shaped burrows at a claystone-siltstone interface in Unit 6 (Pl. 6, fig. 3). These burrows occur in the claystone but the upper ends of the tubes are truncated by siltstone and are infilled with silt-sized sediment. Rapid deposition of storm-generated sediment on a muddy substrate could infill and bury the burrows of vagile or hemisessile benthos.

Icnofossils, domichnid, and fodinichnid-type burrows occur as the only evidence of epibionts and endobionts in the intercalated siltstone and claystone facies. Trace fossils are excellent indicators of specific environmental factors. Seilacher (1964, p. 303) stated that the occurrence of icnofossils in sediments is the best possible proof of non-euxinic or aerobic environmental conditions. Chamberlain (1971, p. 46) reported from his study on the bathymetery and paleoecology of the Ouachita geosyncline that in a marine sequence the occurrence of burrows suggests essentially normal salinity, and attests to continuous environmental hospitality.

Horizontal fodinichnia burrows, present in this facies in Units 2, 4, and 5, are indicative of generally deeper water where the sedimentation rate is slower and muds settle from suspension. Domichnid-type, vertical, U-shaped burrows, as occur in Unit 6, generally indicate a more active environment, shallow water, or tidal areas, where currents were sufficient to provide food and where erosion and sedimentation rates were not detrimental.

The vertical sequence within the siltstone-claystone facies, indicated by the trace fossil occurrence, suggests a transgressive phase for the lower beds, and a shift to a regressive phase in the upper beds, perhaps within Unit 6.

Sandstone Facies.—The sandstone facies of the study area represents sediments deposited during the static and regressive phases of the Oxfordian seaway from east-central Utah. The coarser texture of the facies, in comparison to underlying and overlying rocks, probably reflects the steadily increasing influence of a rising westerly source area (Brenner and Davies, 1974, p. 409), resulting in the rate of detrital sediment deposition surpassing the rate of basin subsidence.

This facies was deposited as a broad sheet of clean sand, which varies in thickness and covers an extensive area. Gilluly and Reeside (1928) measured the entire Curtis Formation throughout the San Rafael Swell and some contiguous areas. The sandstone interval, from 30 to 220 feet thick, comprises a major part of at least seven of their measured sections. Where it was measured in the Green River Desert, south of Green River, Utah, the sandstone facies attains a thickness of 30 feet. Maximum thickness of the facies is observed in sections measured on the southern, western, and northern flanks of the San Rafael Swell, at least 95 km (60 miles) from the Green River section (Gilluly and Reeside, 1928, p. 61).

The sandstone facies involves several geometrical relationships of different scales. The most gross geometrical aspect is the relatively thin but aerially extensive, sheetlike nature of the sandstone interval. Such sheetlike sand bodies may be produced in several ways. Lateral fluctuations of a shoreline in response to numerous minor transgressive and regressive events will produce sand bodies with sheetlike geometries (Rainwater, 1966, p. 11). Boyd and Dyer (1966, p. 172) in their study of the Frio barrier bar system of south Texas, stated that vertical and horizontal growth of a sand barrier results from the rate of regression of the sea. Frio barrier sediments were deposited laterally rather than vertically when regression occurred at a more rapid rate. Laterally significant-sized sand bodies may be created by sea level maintaining relative stability concurrent with a balance between sediment deposition and basin subsidence (Berg, 1954, p. 876). Potter and Siever (1955, p. 444) in their study on stratigraphic variability, stated that sheet sands are related to stable shelf environments and probably result from extensive reworking and low sedimentation rates.

The proposed model for development of the sheetlike Curtis sandstone facies is more consistent with ideas of Berg and of Potter and Siever. Curtis sand deposition began during the initial regression and subsequent narrowing of the Oxfordian seaway. Very shallow water characterized the seaway at that time and sufficient turbulence was maintained to prevent deposition of muds and mixing with the sands. Potter and Siever (1955, p. 444) concluded that deposition of clean sands requires an energy level competent to maintain generally continuous transport of sediment on or near the sea bottom, winnowing away those fine clastic particles.

The rate of regression was apparently sufficiently slow that sea level was relatively stable over an extended time. During the period of stability, a relative balance of sediment influx to basin subsidence was sustained thus allowing uniform deposition of sediment over a broad area. The initial gradient of the substrate upon which the sand was deposited was probably low. The depositional surface was most likely essentially planar. Contact of the sandstone facies with the underlying intercalated claystone-siltstone facies is undulatory but sharp, indicating that sand was deposited uniformly upon a generally even surface.

Within the sand-sheet, smaller-scale geometrical relationships can be recognized. Individual sedimentation units thicken or thin normal to the depositional strike. Units 16, 18, and 19 thicken to the west, in a seaward direction, while Unit 15 thickens to the east in a shoreward direction. Maximum thickening occurs in Unit 19, which thickens at a rate of 1120 cm per kilometer (60 feet per mile). Such a rate of thickening indicates a slope of less than one degree. Mechanisms to account for these sedimentary features include those active during sedimentation and post-depositional processes. Potter and Siever (1955, p. 499) related the variability of sedimentation units within small areas with hydrodynamic factors such as tidal currents, wind waves, and rip currents. Rapid influx and filling by sediments of localized depressions in the offshore environment, where the controlling factors would be both hydrodynamic and topographic, could cause thickness variabilities.

Sedimentary structures such as crossbeds, ripple marks, micro-cross-lamination, and megaripple marks, occur in the sandstone facies. Undulatory small-current ripple marks and lingoid small ripple marks are found in units of this facies. Undulatory small ripples represent a transitory form of ripple between low-energy and high-energy ripple forms (Reineck and Singh, 1973, p. 31). Lingoid small ripples (Pl. 6, fig. 6) are produced at velocities greater than that needed to produce small-current ripples (Reineck and Singh, 1973, p. 31).

Megaripples with superimposed small-current ripple marks occur at the top of Unit 11 and in Unit 14. Those which occur at the top of Unit 11 measure 200 cm crest-to-crest, and 40 cm high, and megaripples in Unit 14 have wave lengths of 8 meters and are 50 cm high. Megaripples originate at elevated energy conditions. Reineck and Singh (1973, p. 10) state that megaripples form because of increases in boundary shear stress and stream energy over those levels required to produce small ripples. Megaripples with superimposed small ripples are caused by smaller shear stress values.

Cross-bedding, as observed in the sandstone facies, is both small-scale, less than 5 cm thick, and large-scale, from 5 cm up to 2 meters thick. Micro-cross-lamination occurs in Unit 22 and is similar in morphology and size to those observed in the Entrada section.

Paleocurrent measurements in this facies display unimodal and bimodal patterns (Text-figs. 2d and 2e). Bimodal paleocurrent directions were observed in Units 8 through 11, 13, 14, 17, and 20. Dominant bimodal azimuthal patterns of N 50° E and S 50° W indicate nearly mutually opposed modes. Azimuth patterns of these bimodal paleocurrents indicate that the current movement was generally parallel with the shoreline of the Late Jurassic seaway (Text-fig. 3), and that the currents which produced them were longshore or littoral currents. Selley (1968, p. 106) following Hulsemann (1955) cites an example of bimodal cross-bedding in the marine Molasse in Schwaben as predominantly reflecting transport by longshore currents.

Units 9, 10, and 20 are distinctive in that the grain sizes are definitely related to paleocurrent directions of crossbeds and ripples observed and measured in these units. Units 9 and 20 have diverse grain sizes and display bimodal current trends to the northeast and southwest. Very fine grained material in these units was transported by currents which moved toward the northeast while fine- and medium-grained material was transported toward the southwest. Unit 10 also exhibits bimodal current trends; however, the grain size-current relationship is opposite that in Units 9 and 20.

Small-scale ripple marks superimposed on megaripples commonly show unimodal current directions, some of which are nearly normal with the more dominant bimodal azimuth trends. Current directions measured in ripple marks at the top of Unit 11 trend N 20° W, and unimodal current directions measured in Unit 14 vary considerably, with a range from N 45° W to N 50° E. Directional trends such as these may indicate that onshore-offshore currents were operative at times. These currents were perhaps tidally influenced. Offshore directed rip currents similar to those described by Shepard, Emery, and LaFond (1941) may have been involved. Rip currents attain high velocities, transport large amounts of sand, and create channels filled with sand waves and megaripples (Ingle, 1966, p. 79). Modern studies of rip currents indicate, however, that they are near-shore phenomena.

Imbricate sandstone lenses of Unit 21 (Pl. 6, fig. 5) are aligned with their long axis at a high angle with the paleoshoreline. These lenses have a NNW-SSE linearity but their continuity along strike is unknown. The lenses overlap one another in imbricate fashion, with younger lenses overlapping and acreating toward the west. Individual lenses are small (Appendix 2) and the internal structure is simple. Crossbeds developed in the basal parts of the lenses indicate current motion was toward the west. Ripple marks exposed on the upper surface of one of the lenses also suggests that current trends were east-west, or predominantly offshore.

Evans (1970) in his study of linear sand bodies of the Viking Formation of southwestern Saskatchewan, describes imbricate overlapping of individual Viking members, with younger members overlapping and prograding at high angles to the shoreline. Evans suggests that deposition of the sandstone bodies is from relatively far-from-shore tidal currents, the imbricate pattern caused by migration of the tidal currents.

The unique occurrence of the Curtis imbricate linear sandstone bodies, restricted to Unit 21, strongly suggests a single-event genesis as opposed to deposition due to rhythmically occurring tidal currents. These sandstone lenses may be the products of separate pulses of a single storm.

Offshore- or longshore-directed storm currents and winds could account for the orientation of the lenses and the current motion trends within them. The imbricate disposition and westward acretion may have resulted from the topography caused by earlier storm-pulse deposits. Several lenses are bounded by 10-cm-thick deposits of silty sandstone with abundant organic fragments. These deposits may represent sedimentation during slack periods between storm pulses when current energy was lowered and finer clastic particles could settle from suspension. Individual lenses appear to tow into the underlying sandstone unit, suggesting that concurrent with the deposition of the imbricate lenses, the floor of the seaway was being eroded by the storm-generated currents.

The incidence of syngenetic glauconite in the sandstone facies has many paleoenvironmental implications. Glauconite occurrence indicates specific limiting factors within the environment. Marine water of normal salinity seems necessary for its formation (Takahashi, 1939, p. 504). In modern sediments, formation of glauconite requires an anaerobic environment with the presence of decaying organic matter and related reducing conditions (Cloud, 1955, p. 486).

Glauconite forms today at moderate to shallow, neritic depths with a favorable range in the upper part of the 10 to 400 fathom interval (Cloud, 1955, p. 490). Temperatures advantageous for its origin vary widely, and Cloud and Barnes (Cloud, 1955, p. 489) concluded that it was "not a reliable temperature index, although it may suggest waters that were not markedly warm." Lochman (1949, p. 56), however, suggested a specific range from 8° to 20° C, temperate to warm conditions.

Parent material necessary for formation of glauconite is not agreed on, but Cloud (1955, p. 490) concludes that the decomposition products of igneous and metamorphic rocks are the most abundant source materials. Galliher (1935) reports that glauconite in Monterey Bay, California, forms at the expense of biotite. A slow rate of sedimentation, or a restricted detrital influx appears to be a requirement for glauconite genesis (Galliher, 1935, p. 1363).

During deposition of the sandstone facies, the water was probably of normal salinity with bottom conditions favoring anaerobic, reducing, and slightly alkaline environments. Shallow, turbulent water, with its attendant ripple and megaripple marks, probably winnowed away those remaining glauconite-forming parent minerals such as biotite, leaving no evidence of their presence in the study section. A slow rate of sedimentation is consistent with the formation of glauconite and with the genesis of a sand-sheet geometry.

Upper Interstratified Clayey Siltstone and Sandstone Facies.—Deposits of this facies of the Curtis Formation are characterized by fine grain sizes: clay, silt, and very fine sand. Spatially, grayish olive clayey siltstone dominates the facies, but is interrupted irregularly by thin interbeds of very fine sandstone. Deposits of this Curtis facies are lithologically similar to and apparently interfinger with tidal flat sediments of the Summerville Formation (Stanton, 1975). The upper interstratified clayey siltstone and sandstone facies is interpreted as sediments deposited in a tidal flat environment.

Sediments in this facies are predominantly grayish olive colored, similar to those of the sandstone facies, and contrast with the red beds of the Summerville sediments above. The color is interpreted as an evidence of marine influence. Thompson (1968, p. 58), in his study of tidal flat sedimentation in the Gulf of California, describes a shift in sediment color from brown in the upper-intertidal environment to gray in the lower-intertidal and offshore mud environments. He relates this color shift to the degree of subaerial exposure of the sediments subsequent to deposition. Exposure for short time periods or not at all characterizes the lower-intertidal and subtidal environments. The gray color of the sediments results from slight reducing and anaerobic conditions created by the dominant marine influence. These Curtis tidal flat sediments are probably analogous to Thompson's lower intertidal deposits.

The vertical sequence of clayey siltstone with interbeds of sandstone in this facies is probably a result of coastal progradation with concomitant deposition of the finer fraction interrupted by periods when the supply of fine particles was curtailed. During these periods, reworking by waves and current action of previously deposited sediments winnowed away the finer fraction, and left veneers of very fine sand. Thompson (1968, p. 108) proposed this model to account for the growth of the coastal mud flats in the Gulf of California.

Sedimentary structures, such as ripple marks and crossbeds, were observed in the sandstone interbeds within the tidal flat facies of the Curtis Formation. Ripple marks are low amplitude with parallel crests, and display north-south current directions. Directional orientation of the crossbeds indicates southward current movement. These current-formed structures were most likely produced during those intermittent periods of reworking and winnowing of the sediments when progradation of the tidal flat was inactive.

Convincing physical and biological evidence supporting a tidal flat interpretation for this facies of the Curtis Formation is scant. The primary evidence is the vertical and lateral lithologic and geographic relationship of Curtis sediments with the more obviously tidal flat deposits of the overlying Summerville Formation.

SUMMARY OF THE DEPOSITIONAL HISTORIES OF THE ENTRADA SANDSTONE AND CURTIS FORMATION

The upper three-fourths of the Entrada Sandstone was deposited in a complex coastal-interdeltaic depositional system under typically low-energy conditions. The sediments are composed primarily of continentally derived clastic material which is characteristically fine grained. Sediment was transported into the depocenter by littoral drift, wave action, tidal processes, and perhaps small rivers.

A succession of four different sedimentary environments occurs in the study area, suggesting subsidence accompanied by transgressive phases, and accelerated sedimentation resulting in regressive phases.

Initial Entrada sediments reflect deposition of the thick sandstone and siltstone facies. A regressive phase commenced as basin subsidence was surpassed by the rate of sedimentation resulting in cyclic deposition of the tidal-deltaic environment. A brief transgressive episode and inundation by probable shallow marine waters is reflected by deposition of a green sandstone. As subsidence slowed, or the rate of sedimentation increased, the green, apparently marine sandstone was overlain by sediments of a beach ridge or barrier environment.

The vertical sequence of sediments overlying the initial beach ridge-barrier material shows a series of transgressive and regressive pulses, accompanied by deposition in either the cyclic tidal-delta environment, or deposition in the sandstone-siltstone, seaward, facies. A second major transgression occurred with attendant deposition of a thin, green, apparently marine sandstone, also overlain by regressive beach ridge-barrier sediments. Sediments of the upper part of the section demonstrate a relatively static condition or balance between basin subsidence and sedimentation rate with deposition of clastic material in the sandstone-siltstone facies.

Entrada deposition ceased with a major transgression of the Curtis Sea into the studied area. The hiatus between cessation of Entrada-type sedimentation and initiation of marine sedimentation at the beginning of Curtis time is represented by a thin basal conglomerate.

The lower member of the Curtis section was deposited during transgression of this last major Late Jurassic epeiric sea. These lower marine units are dominantly claystone, reflecting slow, nearly continuous deposition as the seaway probably reached its maximum depth. Thin interbedded siltstones in this member were most likely produced by occasional storms and high-energy currents.

The middle member is a succession of glauconitic sandstone units similar in internal structures and sedimentary characteristics. These units form a widespread sand sheet produced during the slow, sometimes stable, regressive phase of the Curtis Sea. These marine sandstone units represent deposition in warm, shallow, low-energy waters with intermittent storm activity.

The upper glauconitic sandstone and clayey siltstone member shows a gradual change from dominantly greenish sandstone and siltstone beds, to an interdigitating relationship of thin green siltstone beds and reddish claystone beds, and in the upper part of the section, dominantly reddish sandstone and claystone beds of the tidal flat sediments of the overlying Summerville Formation.

APPENDIX 1

Measured Section of the Entrada Sandstone

Beginning at the base of the eastern end of the easternmost Entrada road cut 150 meters east of milepost 106 on Interstate 70. Units 1 through 26 were measured in this road cut. Units 27 through 57 were measured in the next prominent road cut beginning at milepost 106. Units 58 through 63 were measured in off-the-road exposures north of the interstate beginning three road posts (180 meters) west of milepost 106. Units 64 through 68 were measured in a low-profile road cut six road posts (360 meters) west of milepost 106. Units 69 through 71 were measured along both north and south sides of the westernmost Entrada road cut. Units 72 through 97 were measured in off-the-road exposures beginning seven road posts (430 meters) east of milepost 105 and striking to the northwest and west to the base of the Curtis Formation.

Unit No.	*Description*	*Thickness (cm) Unit*	*Cumulative*
	Top of Entrada Sandstone, base of Curtis Formation.		
97	Siltstone: light to moderate brown; mostly covered high angle slope or vertical cliff; where accessible unit is moderately sorted, quartzose; parts are mottled, perhaps rooted; finely cross-laminated in places; interbedded mudstones occur, up to 35 cm thick.	1100	12462
96	Sandstone: light brown; quartzose, very fine grained, moderate sorting, subrounded to subangular; lower part of unit is small-scale ripple laminated and cross-laminated; upper part rippled, sinusoidal ripple laminations, 50 cm wave lengths, 5 cm high; resistant ledge former.	50	11362
95	Siltstone: light to moderate brown; bedding appears churned, perhaps rooted, with distorted lenses of dark brown clay; small "stone baby" weathering habit; persistent ledge former; upper 25 cm is a recessive grayish red mudstone with thin interbeds of siltstone.	95	11312

94	Interbedded sequence of sandstone, siltstone, and mudstone: recessive beneath prominent "stone baby" unit; sandstone, very fine grained, light brown; mudstone, grayish red, crumbly weathering with lenses of greenish siltstone and organic fragments; siltstone, grayish red, mamillary weathering, hard.	140	11217
93	Siltstone: light brown to moderate brown; massive "stone baby" unit very similar in appearance to Unit 89; recessive in middle of unit.	340	11077
92	Mudstone with interbedded siltstone: grayish red and greenish gray mudstone; light brown siltstone, ripple laminated; upper 5 cm is highly rippled, light greenish gray siltstone; recessive, mostly covered slope.	90	10737
91	Siltstone: light brown; fine grained, quartzose, highly rippled, platy weathering; climbing ripples, current direction N 10° W; forms slope.	70	10647
90	Sandstone: light brown; silty, quartzose, moderate sorting; 5 cm thick recessive mudstone in middle; rippled, finely laminated, ripple wave length 35 cm long; ledge.	45	10577
89	Siltstone: light brown; four members, cyclic repetition; prominent "stone baby" bed; first and third members similar, appear massive, but are subtly cross-laminated; red and white chert masses common, some fill cavities; patches of fine to medium sand; second and fourth members are recessive clayey siltstone and mudstone, grayish red, with chert masses.	590	10532
88	Mudstone: grayish purple, mottled blue gray; very silty; contact with underlying unit undulatory; weathers crumbly to flaky; prominent marker bed, very continuous.	17	9942
87	Sandstone: pale red to light brown; very fine grained, well sorted, quartzose, rounded to subrounded; ledge former with large rounded bosses; prominent "stone baby" weathering; finely cross-laminated in parts; upper 50 cm appears bleached, pale pink grading up to pale purple red.	160	9925
86	Sandstone: pale red, mottled grayish red; very fine grained, clayey; recessive; clay lenses common.	60	9765
85	Sandstone: pale red to light brown; very fine grained; highly cross-laminated and rippled; dominant current directions N 30° E, N 70° E, N 85° E; well exposed asymmetrical ripple marks, wave length of 3 cm, height of 3 mm.	50	9705
84	Mudstone: grayish red; well bedded, fine laminar bedding; flaky weathering.	5	9655
83	Siltstone: pale red to light brown; coarse grained, well sorted, well rounded, quartzose; rounded ledge former; "stone baby" weathering; fine laminar to fine cross-laminar bedding.	60	9650

82	Siltstone to very fine sandstone: light brown to pale red; forms vertical cliff; lower 60 cm is recessive; clay lenses give unit appearance of horizontal bedding; upper part of unit is a clayey siltstone, recessive; grayish red clay in fine laminae, flaky weathering; unit capped by a 2 cm thick grayish red mudstone bed.	120	9590
81	Sandstone: pale red, mottled grayish red; silty, quartzose, very fine grained; appears massive, with no stratification, but contains some fine cross-laminae; 380 cm above base begins a fine-grained sandstone; definite boundary is uneven and irregular; upper part of unit is low slope former, highly rippled; climbing ripple sets 4 cm high; exposed ripple marks have wave lengths of 1 cm and trend N 10° W, N 27° W, N 30° W; crossbeds trend N 25° E.	800	9470
80	Sandstone: light brown to pale red; silty, very fine grained, moderate sorting, well rounded; lower 125 cm is cliff former; rest of unit forms low angle slope; typical "stone baby" weathering in lower part of unit; no bedding or internal stratification; confused lenses occur 125 cm above base of unit, medium to coarse-grained sandstone, grayish pink, well rounded, some frosted quartz grains; near middle of unit sandstone lenses appear to be laminated.	600	8670
79	Sandstone: light brown to pale red, mottled; silty, quartzose, very fine grained, moderate sorting, well rounded; no internal stratification; small lenses or rounded grains of gray chert; forms low rounded cliff.	350	8070
78	Siltstone: light brown to pale red; sandy; flaky, crumbly weathering; mostly covered low slope; red and white masses of nodular chert very common, similar to Units 69 and 70; bedding is indistinct.	700	7720
77	Sandstone: pale brown; very fine to very coarse grained, quartzose, moderate to poorly sorted; base of unit is undulatory with weathered-out clasts of clay; nodules of white chert common near base of unit; large scale, trough-shaped crossbeds characterize this unit; foreset laminae defined by coarser grained sandstone; paleocurrent directions from crossbeds range from 150 degrees to 260 degrees; dominant direction is SW; maximum angle of dip of the foresets is 22 degrees.	200	7020
76	Mudstone: grayish red to light green; silty; contains purplish green confused lenses of siltstone.	90	6820
75	Sandstone: light brown on weathered surface, light olive gray on fresh surfaces; very fine grained, quartzose, micaceous, subrounded to angular; large ripple sets with 40 cm wave lengths.	35	6730

74	Siltstone: grayish red mottled green; sandy, similar to Units 70 and 72; has four distinct members; recessive.	40	6695
73	Siltstone: light brown to grayish red at base; contains lenses of fine- to medium-grained sandstone, quartzose, well rounded, poorly sorted; massive "stone baby" unit; weathers to large semicircular bosses several meters in diameter.	280	6655
72	Siltstone: light brown, mottled grayish red; sandy; very similar in appearance to Unit 70; abundant red and white chert masses; upper part of unit weathers to "stone babies," 20 to 30 cm in diameter; top 5 cm is a flaky mudstone, finely laminated, with green sandstone lenses and red chert.	150	6375
71	Sandstone and mudstone: interbedded, cyclic repetition; sandstone, pale red; very fine grained, well sorted, well rounded; highly rippled, with climbing ripple sets up to 5 cm thick; current directions all to the NE, from N 10° E to N 70° E; forms resistant ledges; mudstone, grayish red, flaky, crumbly, recessive slope formers, some beds rippled and cross-laminated, with current motion to the NE.	115	6225
70	Siltstone: mottled grayish red with numerous irregular and confused lenses of light green, very fine grained sandstone; numerous red and white masses of nodular chert, some up to 2 cm long; lower part of unit is recessive with undulating lenses of grayish red mudstone which appear to be soft sediment deformed; upper 20 cm of unit is prominent ledge of fine-grained sandstone, pale red, quartzitic, 5 percent medium-sized quartz grains, moderate to poor sorting with numerous red and white masses of chert; abundant clay fragments near top of unit; 1-mm- to 5-cm-thick bed of white chert, very continuous, marks top of unit.	250	6110
69	Sandy siltstone: grayish red to pale red; forms prominent ledge; cyclic repetition; lower, middle, and upper 100-cm-thick members weather to large bosses, or "stone babies"; lower member is a siltstone with numerous lenses of fine-grained sandstone; poorly sorted, quartzose, well rounded, with 5 percent medium-sized grains; no internal stratification and the sandstone lenses are contorted, suggesting soft sediment deformation; lower middle and lower upper members are 25 cm thick, and weather to baseball-sized "stone babies"; more recessive than thicker members; numerous dark clay ribbons and abundant red and white chert masses; middle 100-cm-thick member is same as lower member except it contains chert similar to that found in	350	5860

	the thinner members, as well as some fine cross-laminae in the upper part.		
68	Mudstone: grayish red; flaky to nodular weathering; recessive.	35	5510
67	Sandstone: light brown to dark reddish brown; unit divided into three members; lower member is a resistant rounded ledge former, 30 cm thick; bedding is massive, and confused; middle 40 cm of the unit the bedding is contorted with numerous mud clasts; top 15 cm is a pale red to light gray green sandstone with weathered-out rounded mud clasts at base, finely laminated lower part with fine cross-laminae at the top; current motion is toward N 30° E.	160	5475
66	Mudstone and interbedded sandstone and siltstone: lower 15 cm is grayish red mudstone interlayered with light reddish gray to light grayish green sandy siltstone, 1 to 2 cm thick; nodular weathered mudstone with some flaky partings; siltstones are finely laminated; upper part of unit is grayish red mudstone.	35	5315
65	Sandstone: gray green, mottled light reddish brown; very fine grained, contorted mud clasts show soft sediment deformation; lower 6 cm of unit is grayish red cross-laminated siltstone, current direction NNE; ledge former.	30	5280
64	Mudstone: grayish red; interbedded sandstones; well stratified, nodular weathering; recessive with sandstone ledges; sandstones are light grayish green, very fine grained, cross and horizontally laminated; base of unit covered.	150	5250
63	Sandstone: pinkish gray; quartzose, very fine grained, well sorted, well rounded; mostly covered slope; ripple laminated with current trends N 50° E; ripple marks are flat crested, 2 cm wave lengths, trending N 20° W to S 20° E.	600	5100
62	Mudstone: grayish red; recessive, not well stratified; near top of unit is a 2-cm-thick very fine-grained sandstone, finely rippled with current trends E to NE.	50	4500
61	Sandstone: moderate reddish brown; quartzose, fine grained, moderate to well sorted, rounded to subrounded; top of unit shows small-scale cross-laminae trending N 50° E; resistant ledge.	150	4450
60	Sandstone: light brown to dark reddish brown; fine grained, quartzose, moderate sorting, rounded to subrounded, 5 percent medium-sized grains; bedding destroyed, heaved and contorted with numerous clasts of mudstone; unit is recessive and mostly covered.	150	4300

59	Sandstone: reddish gray; quartzose, fine grained, well sorted, rounded to subrounded; lower 50 cm is horizontally laminated; 10-cm-thick zone in middle in which bedding is confused, contorted, with veins of gypsum; lower surface of unit is undulatory; upper part of unit consists of large-scale, 50-cm-high crossbed sets, trending W 10° N; foreset dips 22 degrees.	200	4150
58	Sandstone: gray green, mottled reddish brown; very fine grained, quartzose, interbedded mudstone layers 2 to 3 mm thick; sandstone appears to be rooted or churned; lower part is finely cross-laminated; recessive.	75	3950
57	Sandstone: light grayish green; quartzose, fine grained; lower part is massive; middle and upper parts of unit are highly rippled and cross-laminated; dominant current direction N 30° E; small ripple sets 2 cm high; climbing ripples; mostly covered.	300	3875
56	Sandstone: light pinkish gray; quartzose, fine grained, rounded and moderately sorted, some chert; bedding massive with numerous gypsum veinlets.	200	3575
55	Mudstone: light reddish gray; gypsum veinlets 5 mm thick; nodular to mammillary weathering; slope former.	50	3375
54	Sandstone: light pinkish gray; very fine to fine grained, rounded to subrounded quartz grains, moderate sorting; confused internal stratification, churned; 3 cm thick grayish red mudstone in middle of unit.	10	3325
53	Mudstone: moderate reddish brown; well stratified; flaky to nodular weathering; slope former, mostly covered.	50	3315
52	Interbedded sandstone and mudstone: light pinkish gray sandstone; very fine to fine grained; lower 25-cm-thick sandstone is poorly sorted with some medium sand-sized, frosted grains of quartz and massive bedding; next three 10-cm-thick sandstone interbeds are ripple and cross-laminated with paleocurrent direction to the NE, N 40° E, and S 10° W; upper 50-cm-thick sandstone bed is cross-laminated with paleocurrent direction toward the north to N 20° W, with thin interbedded cross-laminated mudstones; grayish red mudstone, recessive, nodular to flaky weathering, gypsum veinlets and some crystalline gypsum; well stratified to poorly stratified.	150	3265
51	Sandstone: light pinkish gray; quartzose, very fine grained, moderate to well-sorted, well-rounded grains; fibrous gypsum veinlets interweave throughout the unit; internal stratification destroyed; upper	200	3115

	20 cm is bleached to light greenish gray; this unit caps the north-facing roadcut and forms a prominent ledge.		
50	Interbedded mudstone and sandstone: grayish red, mottled light pinkish gray mudstone, recessive, mammillary to flaky weathering; poorly to well stratified; sandstone, light reddish gray to light pinkish gray; three prominent lenticular sandstone bodies characterize this unit; easternmost sandstone lens is flat-bottomed and convex up; middle sandstone lens is flat-topped and convex down; westernmost sandstone lens is flat-topped and convex down, and channels into underlying members of unit; sandstones are rippled with current directions generally to the NE; some N 35° W.	210	2915
49	Sandstone: pinkish gray; quartzose, fine grained, moderate to well sorted, rounded to subrounded grains; angular and rounded clay rip-up clasts near base of unit; 1- to 2-mm-thick gypsum veinlets at base of unit; small ripple laminae with current direction N 50° W; also N 20° W; some soft sediment deformation features; prominent ledge former.	110	2705
48	Mudstone and interbedded sandstone: grayish red lower mudstone; nodular weathering, recessive, 3 cm thick; lower sandstone, grayish red, 2 cm thick, fine grained, moderate sorting; middle mudstone 15 cm thick, grayish red, recessive, nodular with lenses of light gray green irregular gypsiferous siltstone, gypsum veinlets; upper sandstone, light gray green with purple mottling; fine grained, moderate to poorly sorted, rounded to subrounded quartz and chert grains with lenses of medium-grained quartz sandstone, massive bedding; upper mudstone, grayish red, mottled, recessive, nodular weathering, may be bioturbated.	35	2595
47	Sandstone: light pinkish gray; quartzose, fine grained, moderate sorting, well rounded; small gypsum veinlets weave throughout unit; internal stratification destroyed by gypsum heaving; some suggestion of soft sediment deformation.	110	2560
46	Mudstone and sandstone doublet: grayish red mudstone is first and third members of unit; recessive, mamillary to nodular habit; nodules 5 to 7 cm in diameter; 1-cm-thick fibrous gypsum veinlets cut at high angles to bedding; horizontally stratified; lower sandstone is most prominent bed in unit, 30 cm thick, light pinkish gray, slightly mottled; quartzose, very fine grained, well-sorted and rounded grains; numerous small gypsum veinlets	90	2450

	subparallel with bedding; cross-laminated; ledge former; suggests soft sediment deformation.		
45	Sandstone: pale red; quartzose, fine grained, well sorted, rounded to subrounded, red and black chert fragments; 1- to 2-mm-long clay lenses; numerous gypsum veinlets weave throughout unit; veinlets up to 1 cm thick, most less than 1 cm; ripple laminae, climbing ripple sets; perhaps bimodal current directions: dominant current trends toward NE; prominent ledge former.	110	2360
44	Interbedded mudstone and sandstone lenses: moderate reddish brown sandstone and grayish red mudstone; fills channels cut into Unit 43; sandstone lenses are thinner, 5 cm thick, and more numerous than mudstone; west from channels the sandstone lenses interfinger with and lens out in the mudstone; recessive unit.	40	2250
43	Sandstone: light brown to pale red; quartzose, very fine grained, well sorted, rounded to subrounded grains; base is rippled with rip-up clasts; 1-mm-thick veinlets numerous, particularly in middle of unit; unit imbricates to the east until it is channeled out by Unit 44 in a series of three channels; dominant current direction N 60° E; resistant ledge former.	125	2210
42	Mudstone with interbedded sandstone and siltstone: grayish red mudstone; light greenish gray mottled red sandstone and siltstone beds 2 to 5 cm thick; rippled, current motion to NE: this unit channels into Unit 41, forming three channels; laterally, the unit changes facies and grades into dominantly sandstone in the channel fills.	170	2085
41	Sandstone: light brown; quartzose, very fine to fine grained, moderate sorting, rounded to subrounded grains, red and black chert fragments; this unit cut by prominent channels toward the east end of road cut; clay rip-up clasts; soft sediment load structures; interlaced by gypsum veinlets subparallel to stratification; generally massive bedding; prominent ledge former.	140	1915
40	Sandstone: light brown; quartzose, fine to medium grained, moderate sorting, rounded to subrounded, chert fragments; unit is lenticular, continuous to the east, discontinuous and grades into Unit 39 toward the west; massive except where unit appears under channel in Unit 41, then it is cross-laminated and rippled with clay rip-up clasts.	25	1775
39	Mudstone with interbedded siltstones: grayish red mudstone, earthy partings, laminar bedding, weath-	28	1750

	ers to rounded nodules; suggestion of soft sediment deformation.		
38	Sandstone: light reddish brown; silty, quartzose, very fine grained, moderate sorting, subrounded to subangular; numerous organic fragments; indistinct bedding, may be soft sediment deformed; mudstone rip-up clasts near base of unit, derived from Unit 37; soft sediment loading structures at base.	35	1722
37	Mudstone: grayish red, earthy; fibrous gypsum veinlets unit weathers to small nodules.	15	1687
36	Sandstone: light reddish brown; silty, very fine to fine grained, moderate to poorly sorted, subrounded to subangular; organic fragments; fibrous gypsum veinlets.	70	1672
35	Sandstone: moderate reddish brown; silty, quartzose, poorly sorted, rounded to subrounded; fibrous gypsum stringers cut across bedding; bedding is indistinct, shows evidence of soft sediment deformation or gypsum heaving.	50	1602
34	Mudstone: grayish red; crumbly, weathers to small nodules; upper 15 cm is a mottled, grayish orange pink sandy siltstone with 10 percent medium sand-sized rounded quartz grains; crudely cross-bedded.	45	1552
33	Siltstone: light reddish brown; composed of 5-cm-thick beds of siltstone interbedded with grayish red mudstone; cross-bedded, current motion toward N 25° E, N 5° W.	45	1507
32	Mudstone: grayish red, mottled light reddish brown; weathers into small rounded nodules; crumbly, with thin lenses of resistant siltstone.	7	1462
31	Siltstone: light reddish brown; finely rippled, current direction N 40° E to N 50° E; resistant ledge former.	6	1455
30	Siltstone: light reddish brown, mottled light brown; lower 25 cm is massive; middle 10 cm weathers flaky; fine ripple laminae, current direction N 10° E.	37	1449
29	Siltstone: light brownish gray; horizontal 1-mm-thick gypsum veinlets near top and bottom of unit; resistant.	3	1412
28	Siltstone: light reddish brown to grayish green; thin bedded; beds separated by grayish red mudstones; gypsum veinlets.	40	1409
27	Siltstone: pale reddish brown, slightly mottled; very fine grained, well sorted, subrounded; cross-laminated, current direction N 30° E; small lenses of fine sandstone.	40	1369
26	Siltstone: light brown; resistant ledge former; fine ripple laminae with current motion to east.	5	1329
25	Sandstone: light brown; quartzose, very fine to medium grained, moderate to poorly sorted, muddy;	50	1324

	numerous interlacing veinlets of fibrous gypsum; poorly bedded, with contorted bedding near top of unit; lower and upper 5 cm are grayish red mudstone.		
24	Sandstone: light brown; quartzose, very fine grained, muddy, moderate sorting; highly rippled; probable bimodal current motion; east direction dominant; ledge former.	7	1274
23	Mudstone: grayish red to moderate reddish brown in upper unit; nodular weathering; recessive; 1 cm thick fibrous gypsum veinlets parallel to stratification; upper part interlayered with fine- to medium-grained sandstone; sandstone occurs irregularly.	29	1267
22	Sandstone: moderate reddish brown; quartzose, very fine grained, well sorted, red chert fragments, few organic fragments; small-scale ripples trending ENE; forms resistant ledge overlain by 15-cm-thick grayish red mudstone with numerous secondary gypsum veinlets; upper sandstone, grayish green, very fine grained to medium grained, poorly sorted, stratification destroyed by gypsum heaving.	38	1238
21	Mudstone with interbedded siltstone: grayish red mudstone; crudely stratified, flaky to nodular weathering; 1 mm thick gypsum veinlets subparallel to bedding; siltstone interbeds 6 to 15 mm thick, moderate reddish brown to greenish gray; finely rippled in places.	42	1200
20	Sandstone with basal mudstone: pale red, mottled greenish gray sandstone; fine grained, well sorted, subrounded to subangular, organic fragments; highly rippled, current motion N 70° E; mudstone moderate reddish brown, 1 cm thick.	9	1158
19	Sandstone: pale red, quartzose, fine grained, moderately sorted, gray and green chert fragments; intensely gypsum veined; internal stratification destroyed by gypsum veinlets; this unit channels out Unit 18 and channels into Unit 17; clay rip-up clasts occur in the base of channel, with clasts being angular, rounded, and bent.	180	1149
18	Sandstone: pale red; quartzose, fine grained, moderate sorting, subrounded; cross-bedded and rippled, current motion toward the east; earthy mudstone partings in upper part, 3 to 4 cm thick; lower part intensely gypsum veined.	30	969
17	Mudstone with numerous thin rippled sandstone interbeds: grayish red mudstone, soft, flaky, or nodular weathering; pale red to light greenish gray sandstone; ripple laminated, current motion due east.	67	939
16	Sandstone: pale red; quartzose, fine grained, moderate sorting, subrounded; complex ripple sets; soft	23	872

	sediment slumping or convolute bedding; gypsum veinlets.		
15	Mudstone: grayish red; platy, tea leaf weathering; some rippled thin sandy partings in middle of unit, 4 mm to 1 cm thick; current direction N 80° E; recessive.	15	849
14	Sandstone: pale red; quartzose, fine grained, moderate sorting, subrounded; rippled with 3 to 4 cm high ripple sets; current motion to NE; subdivided into 1- to 3-cm-thick mudstone which accentuates ripple surfaces; shrinkage cracks, 1 cm wide; gypsum veinlets.	25	834
13	Mudstone, grading up to siltstone: grayish red to reddish brown mudstone; pale red siltstone; fibrous gypsum lenses; platy weathering mudstone; mud cracks.	7	809
12	Sandstone: pale red; quartzose, fine grained, moderate sorting, subrounded; moderately well stratified with large ripple sets trending due east to N 80° E; small lenses outlined by fibrous gypsum veinlets, 1 to 3 cm thick; forms semiledge.	32	802
11	Sandstone: moderate reddish brown; quartzose, fine grained; highly rippled, with ripple sets 1 to 2 cm high, current direction dominantly N 80° E; upper part of unit is interbedded grayish red mudstone; fibrous gypsum veinlets; well stratified unit; mudstone weathers like grape-stone.	40	770
10	Sandstone: moderate reddish brown, mottled green; quartzose; irregular stratification; clasts of mudstone offset across small faults most likely related to soft sediment deformation.	28	730
9	Mudstone with intervening sandstone: grayish red mudstone, recessive, cyclic occurrence of mudstone, sandstone, and mudstone; mammillary weathering of mudstone; sandstone, light greenish gray, mottled; fine grained, 5-cm-thick resistant bed; cross-laminated with current direction toward the SW; small gypsum veinlets in the mudstone.	15	702
8	Sandstone: moderate reddish brown to greenish gray; quartzose, fine grained; finely rippled and cross-laminated; current direction toward the NE, some bimodal toward the SW; forms semislope.	48	687
7	Sandstone: moderate reddish brown; quartzose, fine to medium grained, subrounded to subangular, red and green chert fragments; moderately well stratified; bimodal ripple current directions, N 30° E, to S 30° W; numerous small secondary gypsum lenses; 1 to 2 mm discontinuous grayish red earthy mudstone horizons; shows evidence of soft sediment deformation; ledge former.	95	639

6	Mudstone: earthy; grayish red; recessive; middle of unit is a light gray green sandstone bed, 1 to 2 cm thick, rippled with current direction N 55° to 60° E.	45	544
5	Mudstone with silty sandstone: moderate reddish brown mottled grayish red; massive, semiledge former; stratification lenticular and slightly contorted; small gypsum laminae.	60	499
4	Mudstone alternating with sandstone: grayish red mudstone, horizontal laminae, well stratified; sandstone, fine grained, shows vertical graded bedding up into overlying mudstone; major recessive unit.	59	439
3	Mudstone: sandy; light brownish gray, mottled as Unit 1; gypsum stringers; jasper (red chert) occurs as 1 to 2 mm nodules; upper part contains organic-rich clay rip-up clasts; 5 percent coarse sand-sized quartz grains and chert occurs in upper part of unit; numerous gypsum veinlets.	50	380
2	Mudstone: grayish red; earthy; lower part recessive; laminar bedding, 1 to 2 cm thick; shows evidence of soft sediment deformation; upper part of unit contains sandstone; moderate reddish brown; quartzose, fine grained, 2 to 3 mm fragments of red and green chert; ripples with NE current direction; gypsum veinlets.	30	330
1	Sandstone: moderate reddish brown, mottled grayish red; quartzose, silty, fine grained, moderate to well sorted, subrounded to subangular; contorted bedding; minor rippling, current motion to SW; white secondary gypsum stringers; red jasper nodules; round circular burrows (?); soft sediment deformation suggested; ledge former.	300	330

APPENDIX 2

Measured Section of the Curtis Formation

Beginning 100 meters south of the east end of the Interstate roadcut, continuing west through the north-facing roadcut then striking northwestward.

		Thickness (cm)	
Unit No.	*Description*	*Unit*	*Cumulative*
	Top of Curtis Formation, base of Summerville Formation.		
26	Sandstone: yellowish gray; quartzose, argillaceous, very fine grained, well sorted; trough-shaped cross-bedding; rounded ledge former.	50	6440
25	Silty claystone: mottled grayish red and grayish olive; slightly calcareous; organic fragments; slope former.	10	6390
24	Siltstone: grayish olive; medium grained, well sort-	10	6380

	ed; laminar bedding; lenses of clay up to 10 mm in length parallel to the bedding.		
23	Siltstone: argillaceous, with numerous 10 to 20 cm thick interbedded sandstone layers; grayish olive siltstone, grayish olive to dark yellow brown sandstone; siltstone calcareous, angular to subrounded grains, moderate sorting, quartz, glauconite, feldspar, muscovite and organic fragments; laminar bedding; very fine-grained sandstone, quartzose, glauconite, organic fragments, thin-bedded, ripple marks and cross-bedding; distorted bedding.	1630	6370
22	Sandstone with interbedded argillaceous sandstone: olive gray; quartzose, friable, very fine grained, moderately sorted; feldspar, glauconite, and organic fragments; laminar to finely bedded; trough-shaped cross-beds; current direction to the west; micro-cross-lamination; forms massive sandstone sheets, 10 to 100 cm thick, interbedded with more easily eroded argillaceous sandstone; randomly occurring lenses of sandstone; grayish brown; very fine grained, moderately sorted; feldspar and glauconite; dolomite cemented; numerous burrows.	2000	4740
21	Sandstone: light olive gray; quartzose, very fine grained, moderately sorted, angular to subangular grains; feldspar, glauconite, and organic fragments; finely laminated bedding; forms imbricate shingles, pulselike, with each pulse 8 meters long and 70 cm thick, divided by silty zones up to 10 cm in thickness; individual pulses sheeting south 80 degrees west, with slope angle of 20 degrees; silty zones contain abundant organic fragments; cross-bedded in the lower parts, finely laminated toward the top.	300	2740
20	Sandstone: light olive gray to greenish gray; quartzose, very fine grained to fine grained, moderate sorting, subangular to rounded; glauconite, feldspar; finely laminated with ripple marks, bimodal current directions, trending northeast and southwest.	75	2440
19	Sandstone: light olive gray to dusky yellow; quartzose, very fine grained, moderate sorting, subrounded to rounded; glauconite; unit thins toward the east, completely disappearing at east end of road cut; finely cross-bedded and rippled, ripple trends N 20° to 25° W; organic fragments abundant.	209	2365
18	Sandstone: light olive gray; quartzose, very fine grained, moderate sorting, angular to subrounded; glauconite; thins toward the east losing one-third of its thickness in 210 meters; lower part is massive, upper 20 to 30 cm is horizontally laminated.	194	2156

17	Sandstone: greenish gray and dusky yellow, in alternating couplets; quartzose, very fine grained, angular to subrounded, moderate sorting; glauconite and organic fragments; couplets 10 to 12 cm thick with cross-bedding having bimodal current directions trending toward the northeast and southwest.	198	1962
16	Sandstone: greenish gray; quartzose, angular to subrounded, moderate sorting; glauconite; 1- to 2-cm-high ripple marks; laminar bedding generally, medium bedding locally; unit thickens toward the west, with thickness varying from 85 cm to 120 cm.	120	1764
15	Sandstone: light olive gray; quartzose, very fine grained; horizontal laminar bedding; intense small-scale cross-bedding; clay concretions, 1 to 3 cm long, elongate and irregularly shaped occur throughout the unit; some crossbeds have superimposed ripple marks trending N 35° E; ripple marks are 3 to 4 cm crest-to-crest with ripple troughs filled with organic matter.	45	1644
14	Sandstone: light olive gray; quartzose, fine grained; glauconite; trough-shaped crossbeds up to 35 cm in height; bimodal current directions with dominant current direction being N 50° E, and subordinant current trends toward the southwest; superimposed ripple marks on megaripples; ripple trends range from N 45° W to N 50° E.	55	1599
13	Sandstone: light olive gray; quartzose, fine grained, subrounded to rounded; glauconite, chert and organic fragments; massive bedding with apparent shingling of bedding to the northeast; 10 cm high ripple marks with bimodal current directions N 50° E to S 50° W; clay lenses abundant; megaripple marks with wave lengths of 8 meters occur along the top of this unit; superimposed small ripple marks on megaripple surfaces, wave lengths of 12 cm, and 1 to 2 cm deep; ripple trend is N 20° W.	310	1544
12	Sandstone: greenish gray with dark yellowish orange thin beds; quartzose, very fine grained, poorly sorted, subangular to subrounded; glauconite and abundant organic fragments along bedding planes.	50	1234
11	Sandstone: dusky yellow; quartzose, very fine grained, moderately sorted, subangular to subrounded grains; glauconite; intensely ripple marked with ripples accentuated by carbonaceous matter; yellow clay lenses abundant in middle of unit; ripple trends are bimodal toward the northeast and southwest; ripple sets up to 1 cm in height but vary in crest-to-crest length from 5 to 10 cm; small	305	1184

	scale cross-bedding with some laminar bedding between crossbed sets.		
10	Sandstone: light olive gray; quartzose, very fine to fine grained, subangular to subrounded grains; glauconite; very abundant organic fragments up to 2 cm long and 3 mm wide; massive; ripple marked, with ripples more well defined by finer grained sands; current transport directions N 50° E with few toward the southwest.	40	879
9	Sandstone: greenish gray to dusky yellow; quartzoze, very fine-grained to fine-grained, subangular to subrounded grains; glauconite; horizontal laminar bedding; unit divided into six individual sets, each set being 10 cm in height separated by ripple surfaces with sooty carbonaceous matter on the ripple surfaces; major current trend is N 35° W and N 60° E with interference ripples trending S 50° W; fine-grained sand was transported toward the southwest and very fine material was moved toward the northeast; upper part of the unit is cross-bedded with bimodal current directions same as those ripple trends in the lower part of the unit.	40	839
8	Sandstone: greenish gray; quartzose, very fine grained to fine grained, subrounded to rounded grains, moderately sorted; glauconite and abundant carbonaceous fragments; complexly lensed with individual lenses up to 30 cm high and 300 cm long with laminae of finer material separating lenses; ripple marks and trough-shaped cross-bedding common; bimodal current directions, N 65° E to N 75° E and S 50° W; rip-up clasts.	67	799
7	Clay pebble conglomerate: yellow gray; poorly sorted; calcareous; clasts up to 10 cm in diameter; discontinuous unit.	10	732
6	Claystone with interbedded resistant siltstone lenses: grayish olive to grayish olive green; laminar bedding; lenticular, highly ripple-marked siltstone lenses; small-scale trough-shaped crossbeds; organic fragments abundant; U-shaped vertical burrows.	180	722
5	Claystone with interbedded resistant siltstone beds: grayish olive to grayish green; laminar bedding in claystone; four lenticular ripple-marked siltstone beds 10 to 25 cm thick divide unit; intensely cross-bedded.	135	542
4	Claystone with interbedded resistant siltstone beds: grayish olive to grayish olive green claystone; dusky yellow siltstone; claystone laminar to massive bedding; unit divided by four lenticular, ripple-marked siltstone beds; trace fossils, burrows, in claystone.	231	407

3	Claystone with interbedded resistant siltstone bed; grayish olive claystone and dusky yellow siltstone; laminar bedded claystone; unit divided by 5-cm-thick finely cross-bedded siltstone; abundant organic matter on bedding planes.	116	176
2	Claystone with interbedded resistant siltstone beds: grayish olive claystone, dusky yellow siltstone; gypsum stringers concordant with bedding; siltstone beds, 1- to 5-cm-thick divide unit, highly cross-bedded; organic fragments abundant on parting surfaces; burrows observed in claystone.	52	60
1	Conglomerate: light olive gray, weathers yellowish gray; calcareous; poorly sorted; rounded and broken rounded clasts up to 6 cm in diameter.	8	8

Base of Curtis Formation and top of Entrada Sandstone.

REFERENCES CITED

Adams, J. E., and Rhodes, M. L., 1960, Dolomitization by seepage refluxion: Bull. Amer. Assoc. Petrol. Geol., v. 44, p. 1912-20.

Bailey, E. H., and Stevens, R. E., 1960, Selective staining of K-feldspar and plagioclase on rock slabs and thin sections: Amer. Min., v. 45, p. 1020-25.

Baker, A. A., Dane, C. H., and Reeside, J. B., Jr., 1936, Correlation of the Jurassic formations of parts of Utah, Arizona, New Mexico and Colorado: U. S. Geol. Survey Prof. Paper 183, 63 p.

Berg, R. R., 1954, Franconia Formation of Minnesota and Wisconsin: Bull. Geol. Soc. Amer., v. 65, p. 857-82.

Bissell, H. J., 1959, Silica in sediments of the Upper Paleozoic of the Cordilleran area: *in* Ireland, H. A. (ed.), Silica in sediments: Soc. Econ. Paleont. Mineral., Spec. Pub. 7, p. 150-85.

Boyd, D. R., and Dyer, B. F., 1966, Frio barrier bar system of south Texas: Bull. Amer. Assoc. Petrol. Geol., v. 50, p. 170-78.

Brenner, R. L., and Davies, D. K., 1974, Oxfordian sedimentation in western interior United States: Bull. Amer. Assoc. Petrol. Geol., v. 58, p. 407-28.

Bundy, W. M., 1956, Petrology of gypsum-anhydrite deposits in southwestern Indiana: Jour. Sed. Pet., v. 26, p. 240-52.

Chamberlain, C. K., 1971, Bathymetery and paleoecology of Ouachita geosyncline of southeastern Oklahoma as determined from trace fossils: Bull. Amer. Assoc. Petrol. Geol., v. 55, p. 34-50.

Cloud, P. E., Jr., 1955, Physical limits of glauconite formation: Bull. Amer. Assoc. Petrol. Geol., v. 39, p. 484-92.

Deffeyes, K. S., Lucia, F. J., and Weyl, P. K., 1965, Dolomitization of recent and Plio-Pleistocene sediments by marine evaporite waters on Bonaire, Netherlands Antilles: *in* Pray, L. D., and Murray, R. C., (eds.), Dolomitization and limestone diagenesis: Soc. Econ. Paleont. Mineral., Spec. Pub. 13, p. 71-88.

Dunbar, C. O., and Rodgers, J., 1966, Principles of stratigraphy: John Wiley and Sons, Inc., New York, 356 p.

Evan, W. E., 1970, Imbricate linear sandstone bodies of Viking Formation in Dodsland-Hoosier area of southwestern Saskatchewan, Canada: Bull. Amer. Assoc. Petrol. Geol., v. 54, p. 469-86.

Evans, G., 1965, Tidal flat sediments and their environments of deposition in the Wash: Quart. Jour. Geol. Soc., London, v. 121, p. 209-45.

Folk, R. L., and Pittman, J. S., 1971, Length-slow chalcedony: a new testament for vanished evaporites: Jour. Sed. Pet., v. 41, p. 1045-58.

Friedman, G. M., 1959, Identification of carbonate minerals by staining methods: Jour. Sed. Pet., v. 29, p. 87-97.

Galliher, E. W., 1935, Glauconite genesis: Bull. Geol. Soc. Amer., v. 46, p. 1351-65.

Gilluly, J., and Reeside, J. B., Jr., 1928, Sedimentary rocks of the San Rafael Swell and some adjacent areas in eastern Utah: U. S. Geol. Survey Prof. Paper 150-D, p. 61-110.
Hamblin, Wm. K., 1961, Micro-cross-lamination in upper Keweenawan sediments of northern Michigan: Jour. Sed. Pet., v. 31, p. 390-401.
Hantzschel, W., 1962, Trace fossils and problematica: *in* Moore, R. C. (ed.), Treatise on invertebrate paleontology: University of Kansas Press, p. W177-W232.
Imlay, R. W., 1948, Characteristic marine Jurassic fossils from the western interior of the United States: U. S. Geol. Survey Prof. Paper 214-B, p. 13-23.
———, 1952, Correlation of the Jurassic formations of North America, exclusive of Canada: Bull. Geol. Soc. Amer., v. 63, p. 953-92.
———, 1957, Paleoecology of Jurassic seas in the western interior of the United States: *in* Treatise on marine ecology and Paleoecology, v. 2, Geol. Soc. Amer. Mem. 67, p. 469-504.
Ingle, J. C., 1966, The movement of beach sand: Developments in Sedimentology, v. 5, Elsevier Pub. Co., Amsterdam, 221 p.
Jopling, A. V., and Walker, R. G., 1968, Morphology and origin of rippledrift cross-lamination, with examples from the Pleistocene of Massachusetts: Jour. Sed. Pet., v. 38, p. 971-84.
Kuenen, Ph. H., and Menard, H. W., 1952, Turbidity currents, graded and non-graded deposits: Jour. Sed. Pet., v. 22, p. 83-96.
Lawyer, G. F., 1972, Sedimentary features and paleoenvironment of the Dakota Sandstone (Early Upper Cretaceous) near Hanksville, Utah: Brigham Young Univ. Geology Studies, v. 19, part 2, p. 89-120.
LeBlanc, R. J., 1972, Geometry of sandstone reservoir bodies: *in* Cook, T. D. (ed.), Underground waste management and environmental implications: Amer. Assoc. Petrol. Geol. Mem. 18, p. 133-90.
Light, M. A., 1952, Evidence of authigenic and detrital glauconite: Science, v. 115, p. 73-75.
Lochman, C., 1949, Paleoecology of the Cambrian in Montana and Wyoming: Natl. Res. Council U. S., Committee on a Treatise on Marine Ecology and Paleoecology, Rept. 9, p. 37-71.
Masson, P. H., 1955, An occurrence of gypsum in southwest Texas: Jour. Sed. Pet., v. 25, p. 72-77.
McCrone, A. W., 1964, Water depth and midcontinent cyclothems: *in* Merriam, D. F. (ed.), Symposium on cyclic sedimentation: Kansas Geol. Survey Bull. 169, v. 1, p. 275-81.
McKee, E. D., 1957, Flume experiments on the production of stratification and cross-stratification: Jour. Sed. Pet., v. 27, p. 129-34.
———, 1966, Significance of climbing-ripple structure: U. S. Geol. Survey Prof. Paper 550D, p. D95-D103.
Miller, W. J., 1952, An introduction to historical geology: D. Van Nostrand Company, Inc., New York, 555 p.
Murray, R. C., 1964, Origin and diagenesis of gypsum and anhydrite: Jour. Sed. Pet., v. 34, p. 512-23.
Petersen, M. S., Rigby, J. K., and Hintze, L. F., 1973, Historical geology of North America: Wm. C. Brown Company Publishers, 193 p.
Potter, P. E., and Siever, R., 1955, A comparative study of Upper Chester and Lower Pennsylvanian stratigraphic variability: Jour. Geol., v. 63, p. 429-51.
———, and Pettijohn, F. J., 1963, Paleocurrents and basin analysis: Academic Press, Inc., New York, 296 p.
Rainwater, E. H., 1966, The geologic importance of deltas: *in* Shirley, M. L., and Ragsdale, J. A. (eds.), Deltas: Houston Geol. Soc., p. 1-16.
Reineck, H. E., and Singh, I. B., 1973, Depositional sedimentary environments: Springer-Verlag, New York, 439 p.
Seilacher, A., 1964, Biogenic sedimentary structures: *in* Imbrie, J., and Newell, N. D. (eds.), Approaches to paleoecology: John Wiley and Sons, Inc., New York, p. 269-316.
Selley, R. C., 1968, A classification of paleocurrent models: Jour. Geol., v. 76, p. 99-110.
Shepard, F. P., Emery, K. O., and LaFond, E. C., 1941, Rip currents: a process of geological importance: Jour. Geol., v. 49, p. 377-69.

Shrock, R. R., 1948, Sequence in layered rocks: McGraw-Hill Book Company, Inc., New York, 507 p.
Stanton, R. G., 1976, The paleoenvironment of the Summerville Formation on the west side of the San Rafael Swell, Emery County, Utah: Brigham Young Univ. Geology Studies, v. 22, part 4, p. 37.
Takahashi, Jun-Ichi, 1939, Synopsis of glauconitization: Trask, P. O., et al., Recent Marine Sediments: Amer. Assoc. Petrol. Geol., Thomas Marby and Co., London, p. 503-12.
Tanner, W. F., 1965, Upper Jurassic paleogeography of the Four Corners region: Jour. Sed. Pet., v. 35, p. 564-74.
———, 1967, Ripple mark indices and their uses: Sedimentology, v. 9, p. 89-104.
Thompson, R. W., 1968, Tidal flat sedimentation on the Colorado River delta, northwestern Gulf of California: Geol. Soc. Amer. Mem. 107, 133 p.
Walker, R. G., 1963, Distinctive types of ripple-drift cross-lamination: Sedimentology, v. 2, p. 173-88.